Advances in Spheroids and Organoids on a Chip

Guocheng Fang, Yu-Cheng Chen, Hongxu Lu,* and Dayong Jin*

Multicellular spheroids and organoids are promising in vitro 3D models in personalized medicine and drug screening. They replicate the structural and functional characteristics of human organs in vivo. Microfluidic technology and micro-nano fabrication can fulfill the high requirement of the engineering approach in the growing research interest in spheroids and organoids. In this review, spheroids and organoids are comparatively introduced. Then it is illustrated how spheroids- and organoids-on-a-chip technology facilitates their establishment, expansion, and application through spatial-temporal control, mechanical cues modeling, high-throughput analysis, co-culture, multi-tissue interactions, biosensing, and bioimaging integration. The potential opportunities and challenges in developing spheroids- and organoids-on-a-chip technology are finally outlooked.

1. What are Spheroids and Organoids?

3D cell culture has now been well-accepted and broad-used since Mina Bissell and her team highlighted the significance of extracellular matrix (ECM) in adjusting the cell behavior while establishing the in vitro cell models in the 1980s.[1] Compared to the 2D monolayer culture, where cells adhere to the surface of a plate, 3D cell culture allows cell growth and interactions with surroundings in all directions, which mimics the specificity and homeostasis in vivo.[2] Accordingly, the 3D cell models remain relatively high similarity to the real tissues in terms of cell differentiation, drug resistance and metabolism, and stimulus-response. The global market size of 3D cell culture is valued at $1.66 billion in 2021 and is projected to reach $6.46 billion by 2030, at a CAGR of 16.3%.[3]

Multicellular spheroids and organoids are the leading representative models in 3D cell culture. Spheroids usually refer to the well-rounded and compacted cell aggregation that usually consists of a single type of cells (epithelial, mesenchymal, endothelial, etc.).[4] They could be formed by the cell lines, single cells, or crypts from the tissues via biopsy (**Figure 1**). Different types of cells can also be mixed to form the randomly-distributed or cell type-based hierarchic spheroids. The spheroid formation can be divided into two stages: 1) formation of loose cell aggregates via integrin-ECM binding by constraining the cells in a confined space (e.g., round-bottom wells); 2) formation of compact spheroids via cadherin expression, accumulation and interaction.[5] Many reviews have summarized the formation techniques of multicellular spheroids.[6]

From a microscopic view, when the solid tumor gets larger, the increased distance to blood vessels depresses the metabolism of the tumor cells.[7] According to the proliferation rate, a solid tumor can be divided into a proliferative zone, quiescent zone, and hypoxic zone. Consequently, there form chemical gradients (pH, oxygen, glucose, ATP distribution, lactate accumulation, etc.). The cells in various zones respond to the drug differently, which is one of the main reasons for drug resistance.[8] The hierarchic layout and chemical gradient can be observed in multicellular tumor spheroids with a decreased proliferation rate from rim to core. Moreover, the spheroids can secret similar ECM molecules.[9] These promise the multicellular tumor spheroids of well mimicking the solid tumor.

The current definition of an organoid is a 3D structure grown from stem cells and consisting of organ-specific cell types that self-organize through cell sorting and spatially restricted lineage commitment.[10] Before 2005, the word organoid was an extension of 3D culture.[11] The stem cells can originate from the adult stem cells (aSCs) derived from the dissociated tissue samples (single cells or crypts). Another type of stem cell is the pluripotent stem cells (iPSCs) and pluripotent embryonic stem cells (ESCs). These cells are usually embedded in the matrix gel to maintain self-organization. Some research mistakes

G. Fang, Y.-C. Chen
School of Electrical and Electronics Engineering
Nanyang Technological University
50 Nanyang Ave., Singapore 639798, Singapore
G. Fang, D. Jin
Institute for Biomedical Materials and Devices
School of Mathematical and Physical Sciences
University of Technology Sydney
Broadway Ultimo, Sydney, NSW 2007, Australia
E-mail: dayong.jin@uts.edu.au
H. Lu
State Key Laboratory of High Performance Ceramics and Superfine
Microstructure, Biomaterials and Tissue Engineering Research Center
Shanghai Institute of Ceramics
Chinese Academy of Sciences
1295 Dingxi Road, Shanghai 200050, China
E-mail: hongxu.lyu@mail.sic.ac.cn
D. Jin
UTS-SUSTech Joint Research Centre for Biomedical Materials & Devices
Department of Biomedical Engineering
Southern University of Science and Technology
Shenzhen 518055, China

The ORCID identification number(s) for the author(s) of this article can be found under https://doi.org/10.1002/adfm.202215043.
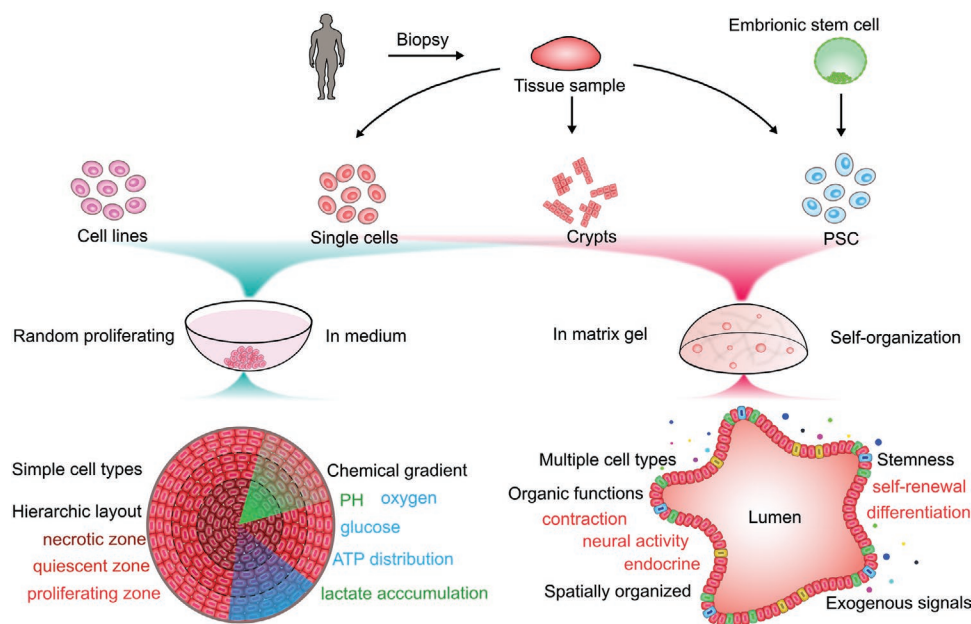
Figure 1. Schematic establishment of spheroids and organoids and their characteristics. Spheroids are developed (usually in medium) from simple cells, with random proliferation, solid and hierarchic layout, and chemical gradient. Organoids are usually derived from stem cells (aSCs, iPSCs, ESCs) embedded in matrix gel and supported by exogenous signals. They contain multiple cell types with high polarization and certain organic functions.

the multicellular spheroids as organoids. The most intuitive difference is that the multicellular spheroids mimic the chaotic proliferation of a cell cluster, while the organoids are highly-ordered and polarized 3D structures, and some have the typical lumens (gastrointestinal organoids, lung organoids, etc.). The organoids contain multiple cell types and have self-renewal and differentiation supported by exogenous signals.[12] They show similar organ functions, for instance, periodic contraction (cardiac organoids), neural activity (brain organoids), and endocrine secretion (mammary gland organoids).

To date, more than 15 kinds of organoids have been successfully established via aSCs, iPSCs, or ESCs, such as the brain organoid, retina organoid, stoma organoid, liver organoid, kidney organoid, intestine organoid, pancreas organoid, prostate organoid, endometrium organoid, etc. It should be noted that the various relevant tumor organoids have also been established. Organoids are now widely used in organogenesis, pathogenesis, drug discovery, personalized medicine, disease models, etc.

2. Overall Advances of Spheroids and Organoids on a Microfluidic Chip

Reproducing and optimizing the microenvironment is the tenet to establish the in vitro multicellular spheroids and organoids. In conventional culture, the formation of spheroids and organoids relies on random self-assembly or self-organization in the medium or matrix, lack of the stimulus, such as chemical gradient and mechanics, which are common in in vivo microenvironments. Therefore, engineering approaches are required to improve the successful culture of spheroids and organoids in vitro.

With the development of micro-nano fabrication, microfluidic technology becomes a valuable tool to address the issues in the conventional culture of spheroids and organoids. The microfluidic device can constrain the fluids to a small scale, matching the size of spheroids and organoids. Small volume control enables the microfluidic with low sample consumption, and microdomain effects, facilitating observation and analysis. The integration of micropumps and microvalves could further accelerate automation and industrialization. Indeed, there has been a growing trend of combining spheroids and organoids with the on-chip technology in the last few years.[13] Some articles reviewed the spheroids- and organoids-on-a-chip technology based on the organ type,[14] specific biofunctions,[15] or specific microfluidic techniques, such as microfluidic droplets.[16] In this review, guided by the characteristics of on-chip technology, we summarize the recent advances of spheroids and organoids on the chip contrastively. As shown in **Figure 2**, in general, the microfluidic technology could facilitate the establishment of spheroids and organoids in the following aspects: 1) spatial-temporal control; 2) mechanical cues modeling; 3) high-throughput analysis; 4) multi-tissues or organs interaction; and 5) integration of biosensing and bioimaging.

2.1. Spatial-Temporal Control

2.1.1. Chemical Signals

The organogenesis from stem cells to organoids requires the biochemical stimulus from exogenous signals, also called the morphogens, such as the bone morphogenetic protein 4 (BMP4), proto-oncogene protein (WNT3), and Noggin. It is critical to understand the exact functions of each morphogen in
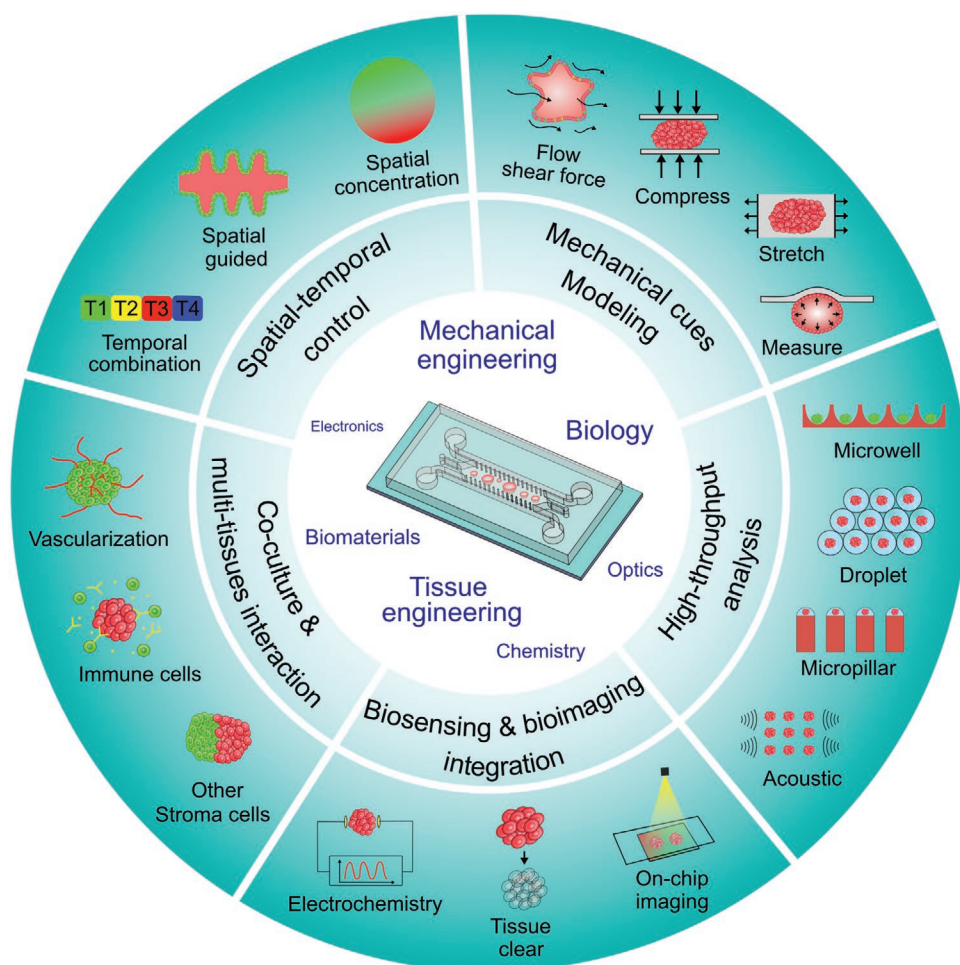
2215043 (2 of 19)

Figure 2. Overall advances of spheroids and organoids on a chip. Microfluidic chip enables spatial-temporal control, mechanical cues modeling, high-throughput analysis, multi-tissues or organs interaction, biosensing, and bioimaging integration.

organ development. In the conventional culture of organoids, the stem cells or pre-formed organoids expose to a uniform concentration of these morphogens, leading to the radially symmetric spatial organization. This, on the one hand, deviates from some asymmetric development in vivo. On the other hand, it may obscure the real function of the morphogens.

Spheroids- and organoids-on-a-chip technology could control the spatial distribution of the morphogens, magnifying the response and revealing their functions.[17] The most common strategy is the gradient-concentration model, utilizing the molecule diffusion on the chip or in the matrix. As shown in **Figure 3**A, a microfluidic device for exposing human stem cells to a localized morphogen source is fabricated. The cell chambers were separated from external perfusion channels by barriers formed from inner polyethylene glycol (PEG) hydrogel. A concentration gradient (red-labeled dextran) can be generated in the cell chamber, following the source–sink model of Fickian diffusion. The nonuniformed exposure leads to the asymmetric expression of pluripotency markers (MIXL1, SOX2, etc.) in human ESCs. This engineered signaling helps to investigate the self-organization of stem cells. A similar device was also used to study the heterogeneous response of a colorectal

tumor to gemcitabine-loaded dendrimer nanoparticles,[18] the neural tube development in a WNT gradient by the gradient generator.[19] The hydrogels include natural hydrogels (such as alginate, agarose, gelatin, hyaluronic acid, collagen, Matrigel, etc.) and artificial hydrogels (such as PEG, hydrophilic poly (ethylene glycol) diacrylate) (PEGDA), etc.). Different agents, such as small molecules, proteins and nanoparticles, showed different diffusion patterns and rates. Luckily, they all can successfully form gradient concentration.[20]

For the spheroid investigation, more work is focused on the spatial control of the concentration of drugs and nutrition.[21] The most common strategy is the combination of a concentration gradient generator with a microwell array or microdroplet array (Figure 3B). By increasing the inlets and extending the spheroid culture array, multiplexed drug combinations (8 drugs and 172 conditions) could be achieved on the chip.[22]

Except for the spatial combination of the drug, spheroids- and organoids-on-a-chip technology enables the time-sequential drug combination.[23] As shown in Figure 3C, the human pancreatic ductal tumor organoids are cultured in the microwell layer and irrigated by the medium in the top channels. The microvalves configured on the chip automatically provide the
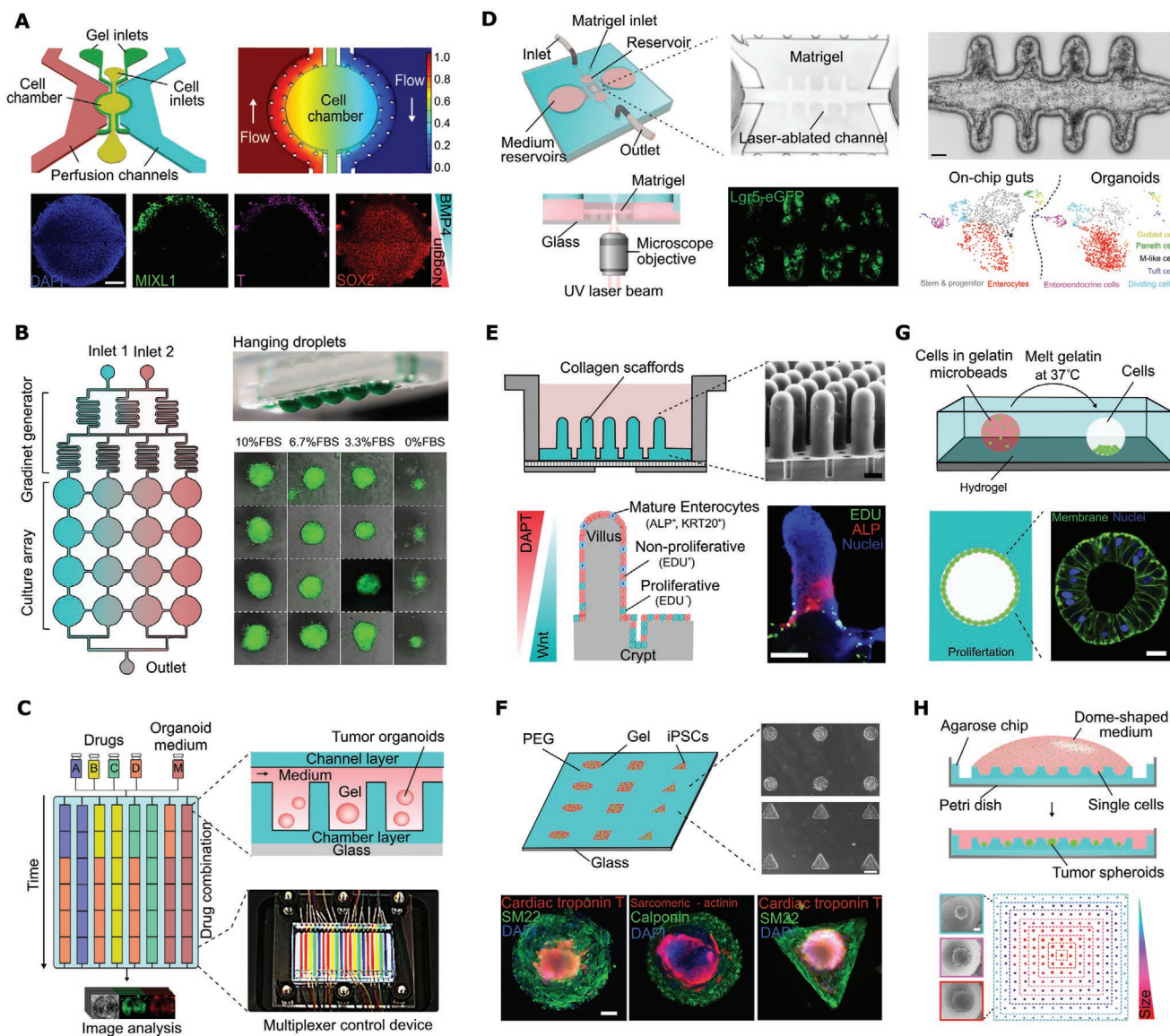
Figure 3. Spatial and temporal control on the microfluidic chips. A) Differentiation of stem cells exposed to morphogens with a concentration gradient following the source-sink model. Human ESCs could form asymmetric pluripotent expression. Scale bar:200 µm. Reproduced with permission.[17a] Copyright 2019, Nature Publishing Group. B) Droplet array combined with the concentration gradient generator to investigate the growth under different dosages of nutrition or drugs. Reproduced with permission.[21c] Copyright 2014, Nature Publishing Group. C) Temporally-modified drug treatment in the organoids on a chip. Reproduced with permission.[23a] Copyright 2020, Nature Publishing Group. D) Scaffold-guided spatial control of the morphology of the intestinal organoids. The Matrigel channel was ablated by the laser. Scale bar:50 µm. Reproduced with permission.[25a] Copyright 2020, Nature Publishing Group. E) Polarized differentiation of the intestinal epithelium induced by the crypt-villus-shaped scaffold. Scale bar:100 µm. Reproduced with permission.[30a] Copyright 2017, Elsevier. F) Micropattern-based investigation of early cardiac organoids. The pattern is usually fabricated by light-activated hydrogels via a photomask. Scale bar: 100 µm. Reproduced with permission.[32] Copyright 2018, 2015, Nature Publishing Group. G) Hollow spheroid formation via the gelatin sacrificial method. Scale bar: 20 µm. Reproduced with permission.[36] Copyright 2017, Elsevier. H) Gradient-sized spheroids on a single chip guided by the dome-shaped culture medium. Scale bar: 50 µm. Reproduced with permission.[37] Copyright 2019, Royal Society of Chemistry.

temporally-modified drug treatments, allowing high efficiency than constant-dose monotherapy or combination therapy.

2.1.2. Morphology Guidance

Spheroids- and organoids-on-a-chip technology could reproduce and optimize the intrinsic morphology shown in vivo.[24]

For instance, the epithelial organoids developed in the matrix gel usually form closed and cystic structures. Although bud sprouting occurs on the mature organoids, these organoids maintain a considerable gap with the real organs in size, lifespan, and morphology. As shown in Figure 3D, the on-chip technic formed millimeter-scaled and tube-shaped intestinal organoids with the crypt-and villus-like domains, guided by the scaffold shape.[25] The laser-ablated Matrigel channel assists the

self-organization of organoid cells, which could also be connected with the external pumping system for continuous perfusion. The guided intestinal organoids prolonged their lifespan for several weeks and contained rare cell types that are less observed in unguided organoids. Similar spatial expansion can be achieved by 3D bioprinting technology for gastrointestinal organoids[26] and human brain organoids.[27] Spatial fusion of the luminal airway organoids is also conducted via the Poly-dimethylsiloxane (PDMS) mold guidance, achieving tubular expansion.[28]

The designed topography can conversely create the source-sink biochemical gradient via morphology, which induces the homogeneous differentiation of the organoids.[29] A presentative model (Figure 3E) shows that the engineered crypt-villus-shaped collagen scaffold can form a vertical concentration gradient of the gamma-secretase inhibitor DAPT and WNT during the culture of intestinal epithelium cells. Notably, the gradient concentration maintained a stem cell-progenitor cell zone and promoted cell migration along the crypt-villus axis, replicating an in vivo phenomenon.[30] High-resolution 3D stereolithography can also replicate the topography of the crypt and villus, such as the Caco-2 model.[31]

Similarly, spatial-induced differentiation can study the early development of cardiac organoids on gel-based micropatterns.[32] As shown in Figure 3F, the geometric-confined human iPSC cells showed different differentiation following the spatial patterning, such as higher OCT4+ and SM22 expression at the perimeter and higher cardiac troponin T and sarcomeric α-actin expression at the central. This could serve as the embryotoxicity assay. The on-chip micropattern strategy can also help to investigate the tubulogenesis in epithelial organs,[33] cell migration[34] and differentiation of mesenchymal stem cells.[35]

Spatial-guided morphology was also used to investigate spheroids. For instance, the intrinsic-achieved spheroids hardly model some luminal tissues. As shown in Figure 3G, a gelatin sacrificial method helps to form the hollow core in lens epithelial spheroids.[36] The gelatin microbeads with the cells inside were embedded in another hydrogel. After melting the gelatin at 37 °C, the cells sedimented at the bottom of the hollow chamber and then grew along the inner surface to form a hollow spheroid. Except for the architecture, the size of the spheroids could also be tunable via the on-chip spatial control.[38] As shown in Figure 3H, a simple method was presented to generate gradient-sized breast tumor spheroids on a single chip.[37] The cell suspension was dropped on a microwell-array chip and then formed a dome-like shape due to the surface tension. After cell sedimentation, microwells at the central contained more cells and that at the edge had fewer cells, resulting in the position-dependent distribution of spheroid size. Moreover, the shape of the spheroids could also be controlled, for instance, geometric-guided by hydrogel templates via the digital micromirror device-patterning.[39] Investigation of the spheroid architecture facilitates the research on tissue engineering and drug delivery.

2.2. Mechanical Cue Modeling

Cells and tissues in vivo live in a 3D microenvironment composed of various biochemicals and dynamic mechanics. Physical mechanics regulate cell behaviors and fates, especially in the developmental process.[9b,40] These mechanic forces include the shear force of haemal or humoral perfusion, expansion stress of pulmonary alveoli, contraction stress of heart beating or myokinesis, etc. Many diseases are related to the disorder of the mechanics, such as coronary calcification and pseudo-obstruction. Unfortunately, in the conventional culture of spheroids and organoids, the microenvironment lacks mechanical cues, deviating from the natural tissues in vivo.

2.2.1. Shear Force from Flow

Spheroids- and organoids-on-a-chip technology could incorporate the shear force of the fluidic perfusion due to the intrinsic advantage of microfluidic. Parameters of flow speed, flow direction, renewal frequency and flow pattern (laminar, vortex, and turbulence) can be controlled well. Flow can enhance the mass transfer and active some mechano-proteins for more functions, such as the Piezo 1 that is sensitive to shear stress in the endothelium.[41] Research has witnessed significant improvement in spheroids and organoids by fluidic shear force.[42] For instance, as shown in **Figure 4**A, the vascularized kidney organoids cultured under flow stimulus grew more podocyte and tubular compartments with increased polarity than those under static culture.[43] After about 10-day perfusion, the shear force induced more endothelial progenitors and perusable lumens, critical architecture for the kidney's filtering function. Another work indicated that the flow-stimulated human islets in the microwells expressed more hair-like microvilli, tighter cell-cell junctions and higher insulin secretion than those under static culture (Figure 4B).[44] During the perfusion, the flow rate can be a two-edged sword. When the flow rate exceeded a certain value (25 µL h^{-1}), the improvement was reduced. Considering the optimal flow rate (4.27 mL min^{-1} = 256.2 mL h^{-1}) in the culture of the vascularized kidney,[43] the optimal flow rate varies when culturing different types of spheroids and organoids.

Archenteric organs, such as the esophagus, stomach, and intestine, suffer from the mechanical stimulus induced by the movement of the chyme. However, the conventional-established gastric or intestinal organoids form the closed lumens, which hinders the mimicking of intraluminal mechanics. As shown in Figure 4C, Kang et al. established the stomach-on-a-chip with the micropipette inside to mimic the luminal flow. The flow system was controlled by a peristaltic pump, which could further introduce the stretch and contraction to the organoid.[45] Basolateral convective flow was proved to manipulate the morphologies of 3D-cultured Caco-2 on an orbital shaker.[46]

Brain organoids (e.g., forebrain or midbrain organoids) can also positively respond to the flow-stimulated culture due to the enhanced shear force stimuli, nutrition and oxygen supply.[47] As shown in Figure 4D, a cascaded mini-stirrer driven by a gear-motor system was integrated with the culture of brain organoids. The brain organoids cultured without external control usually lack specificity and contain diverse cell types in the forebrain, hindbrain, and retina. This platform could increase the specificity of the achieved brain organoid and
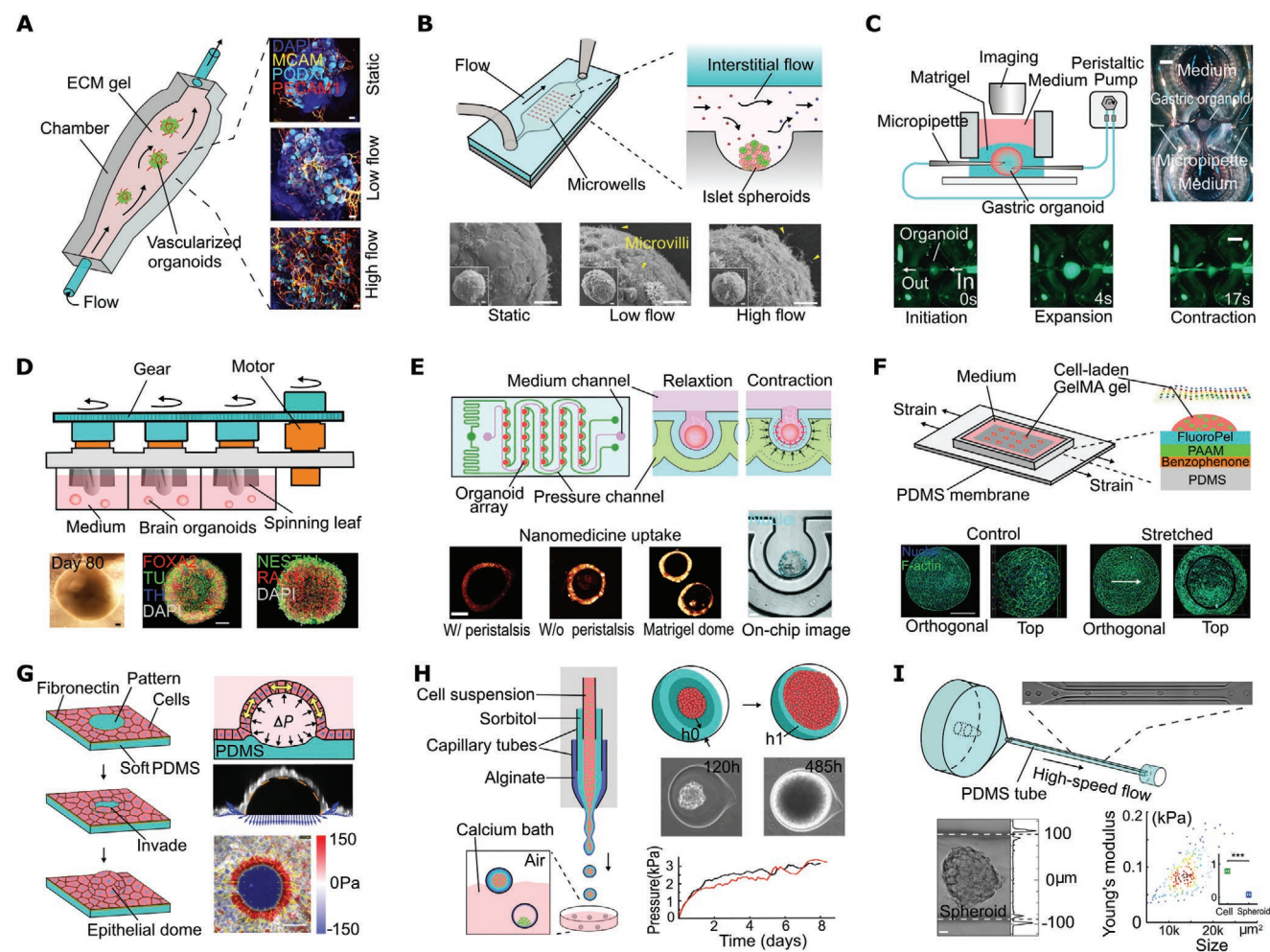
Figure 4. Mechanical modelling and measurement on the microfluidic chips. A) Flow-enhanced vascularization and maturation of kidney organoids. Reproduced with permission.[43] Scale bar:100 µm. Copyright 2019, Nature Publishing Group. B) Flow-enhanced culture of human islet spheroids on the microwell-array chip. Scale bar: 10 µm. Reproduced with permission.[55] Copyright 2019, the American Association of the Advancement of Science. C) Luminal flow in gastric organoids controlled by a peristaltic pump. Scale bar: 2 mm. Reproduced with permission.[45] Copyright 2018, Royal Society of Chemistry. D) Brain organoids cultured on the mini-stirrer system driven by the 3D-printed gear and motor. Scale bar: 200 µm (left) and 100 µm (right). Reproduced with permission.[48] Copyright 2016, Elsevier. E) Human colon tumor organoids contracted on the chip to mimic intestinal peristalsis. Scale bar: 50 µm. Reproduced with permission.[52] Copyright 2021, IOP Science. F) Multicellular spheroids cultured on the PDMS membrane applied periodical stretch. Scale bar: 200 µm. Reproduced with permission.[53] Copyright 2020, Wiley-VCH GmbH. G) Measurement of luminal pressure and tension via the epithelial lumen on the PDMS chip. Scale bar: 50 µm. Reproduced with permission.[56] Copyright 2018, Nature Publishing Group. H) Alginate capsules as a tool to investigate the compressive stress generated by the spheroids. The pressure could be up to more than 3 kPa. Reproduced with permission.[57] Copyright 2013, the National Academy of Science. I) Spheroids-on-chip cytometer for Young's modulus investigation under hydrodynamic stress. Scale bar: 20 µm. Reproduced with permission.[58] Copyright 2020, Nature Publishing Group.

further avoid the waste of medium, recapitulating the key features of human brain development.[48] The brain organoids can be further attached to a 3D-printed resin motor for higher mechanics.[49]

2.2.2. Tension and Compression

Cells and organs in vivo suffer from surrounding strain and stress, which regulate their fate, attracting much mechanobiology research.[50] Spheroids- and organoids-on-a-chip technology could well apply the strain and stress on a flexible substrate (such as PDMS) and open-operability. Representative

research is that Lgr5+ intestinal stem cells can be significantly affected by compressive stress. The Lgr5+ cells self-renew along the crypt-villi axis, resulting in physical heterogeneity via cell expansion. Yiwei et al. established the intestinal organoids in the compressed Matrigel by weight. Under compression, organoids showed upregulated expansion (higher expression of Lgr5 and Ki67).[51] It is also proved this phenomenon results from the crowding of WNT/β-Catenin signaling via compression. This may be associated with the peristalsis microenvironment of the intestine. As shown in Figure 4E, a colon tumor organoid chip containing the medium channel and pressure channel was designed to mimic intestinal peristalsis.[52] The colon tumor organoids can grow in the microwell array

separately and get contracted periodically. Results indicated that the organoids under peristalsis showed obviously reduced uptake of the ellipticine-loaded micelles. Thus, it is supposed that human colon tumor organoids under mechanical stimulus may show different drug resistance. A stretchable microarray for NIH 3T3 fibroblast spheroids is developed utilizing the flexible PDMS/PAAm (polyacrylamide), as shown in Figure 4F. The cell alignment and spreading behaviors were significantly influenced by the tension stimuli.[53] It is also illustrated the HCT116 colorectal tumor spheroids in a confined condition would not impair cell rounding but negatively affect the mitotic progression by altering spindle polarity.[54]

2.2.3. Mechanics Measurement

Mechanical cues generated by spheroids and organoids can be, in turn, measured on the chip. Luminal pressure and tension of epithelial organoids and tissues are critical for developmental defects, inflammatory conditions, and cancer.[59] As shown in Figure 4G, Ernest et al. developed an epithelial lumen-on-a-chip device to measure the luminal pressure and tension according to the deformation of the PDMS substrate. The surface of the PDMS was coated with fibronectin, where epithelial cells could attach, except for the uncovered patterns. With cell proliferation, the lumen will form on the patterns. Surprisingly, the luminal sheet was found to be an active super-elastic material with cellular areal strain up to 1000%.[56]

Compared to healthy tissue, tumor shows different mechanical features (stiffness, interstitial fluid pressure, etc.) due to their high proliferation and secretion.[60] Tumor also generates expanding physical force when their mass is fast increasing, which can affect the tumor biology by directly compressing the surrounding cells. The expansion force is gradually accumulated with the size increase of the tumor. When the tumor reaches a specific size, the escalating compression can reduce the tumor cell proliferation and induce apoptosis, potentially increasing invasion and metastasis. Additionally, these mechanical features vary according to their positions.[61] Mechanical behaviors of tumor spheroids and organoids promote the fundamental mechanobiology study and mechano-guided drug screening. Microfluidic chips could help to encapsulate murine colon tumor CT26 cells inside alginate capsules (Figure 4H). The cells in the permeable capsules formed spheroids and generated pressure on the alginate shell. The alginate could be treated as an elastic material. By analyzing the decreased thickness of the shell, the compressive force in spheroids could be measured. The expansion pressure was found up to 3 kPa.[57] Similarly, Guocheng et al. measured the luminal mechanics of the mouse mammary tumor organoids based on the alginate microbeads. The monolayer lumen can generate ≈2 kPa pressure during their morphogenesis expansion in alginate.[62] In addition, the hydrodynamic force has been widely used to investigate the mechanics of single cells.[63] It can also play a role in the mechanical measurement of spheroids and organoids. As illustrated in Figure 4I, the HEK293T spheroids were introduced into a PDMS flow cytometry to investigate their Young's modules under the hydrodynamic stress. This allows the high-throughput analysis, which showed the average Young's modulus of the HEK293T spheroids was a factor of ten smaller than single cells.[58]

2.2.4. Biomaterials on the Chip

The development of some spheroids and most of organoids usually requires hydrogel support, which offers physical support, mechanical cues and even cell binding sites.[64] Tumor-derived basement membrane extract (BME) is the most widely used material for organoid culture, which is usually available as the commercial products Corning Matrigel® or Cultrex BME2®. The BME-based hydrogel comprises various ECM proteins, proteoglycans, and some growth factors secreted by Engelbreth-Holm–Swarm murine sarcomas.[65] Although this hydrogel has been widely used, it still remains some drawbacks, such as undefined components, high cost, batch-to-batch variation, and great limitations in mechanical features and gelation conditions.

Therefore, it is significant to find the defined substitutes in BME that support organoid establishment. Nicolas et al. find that soft fibrin matrices can provide suitable physical support, similar to the Arg-Gly-Asp (RGD) adhesion. Meanwhile, laminin-111 is the key parameter required for robust epithelial organoid formation and expansion.[66] Additionally, artificial matrices have been synthesized for the expansion of intestinal organoids, such as PEG-based hydrogels and nanocellulose-based hydrogels.[67] Indeed, the stiffness governs their expansion. It is found that the mouse intestinal organoids could form more colonies in PEG-based hydrogel with a stiffness of 1.3 kPa to 1.7 kPa. The degradability of the matrix also influences the phenotype of organoids.[68] Recently, the native non-adhesive alginate has been found suitable for the culture of mouse mammary tumor organoids and human intestinal organoids by embedding cell aggregates inside.[62,69] It is noticed that the decellularized ECM of a specific organ could offer prodigious organ-specific cues for the related organoids,[70] even the organ-specific metastases.[71]

The integration of biomaterials into microfluidics is essential for the development of spheroid- and organoid-on-a-chip technology. The common biomaterials (such as Matrigel, decellularized ECM, collagen, alginate, etc.) could be well introduced into the PDMS-based microfluidic structures (channels, microwells and membranes) and form the gelated hydrogel to support the spheroids and organoids. For instance, the decellularized human brain ECM was integrated into a dynamic microfluidic chip for the reconstitution of the brain microenvironment, allowing the establishment of brain organoids.[72] The ECM sheet could be directly formed on the microfluidic chip by culturing the mouse embryonic fibroblasts inside and then the decellularization. It illustrated compositional heterogeneity and microstructural architectures.[73] It should be mentioned that the natural ECM (such as Matrigel and collagen) usually suffer fragile mechanical features, which challenges the long-term culture of spheroids and organoids on the chip, especially on the dynamic microenvironment, such as high-flow perfusion and periodical stretch. Therefore, it is highly requested to synthesize artificial biomaterials with excellent stability that suit long-term culture.

**ADVANCED
SCIENCE NEWS**

www.advancedsciencenews.com

**ADVANCED
FUNCTIONAL
MATERIALS**

www.afm-journal.de

2.3. High-Throughput Analysis

A reliable conclusion requires a mass of experimental data and samples. High-throughput generation and analyzing capability of spheroids and organoids can help to reduce the contingency and variability. This is crucial for biological experiments and clinical tests where many parameters and processing steps are involved. The spheroids- and organoids-on-a-chip technology has considerable advantages in high-throughput analysis.

2.3.1. Microwells

Microwell is the most widely used tool in 3D culture, especially for spheroids.[74] The microwell array is usually generated by the hydrogels (agarose, gelatin methacryloyl (GelMA), etc.) with pillar stamps, polyester plastics with micro-drilling, or 3D printing, which could increase the yield and control the size.[37–38,44,75] As for the organoids, most types of organoids (e.g., intestinal organoids, gastric organoids) require hydrogel support, which hinders their culture in microwells due to the problematic manipulation of hydrogels. One method is the lateral microwells combined with medium channels.[76] The hydrogel in the channel can be removed. Another method is the bottom microwells integrated with the top perfusion layer.[23a] It should be mentioned that, as shown in **Figure 5**A, the PEG hydrogel microwell array was designed for large-scale suspension development of gastrointestinal organoids.[77] The

researchers replaced the solid Matrigel with the ENR-CV expansion medium containing 2% v/w soluble Matrigel during the beginning 60 h and the differentiation medium in the later culture. The absence of the solid matrix simplified the microwell-array culture and further reduced organoid heterogeneity. Additionally, the islet organoids derived from the iPSCs can grow without matrix and have successfully been combined with microwell.[78]

2.3.2. Droplet and Microbeads

The droplet technique, one of the most representative tools in microfluidics, can generate droplets or microbeads in a high-throughput way,[79] promising the scalable establishment of spheroids and organoids. Some spheroids have been successfully formed in mono-dispersed natural hydrogel (alginate, agarose, etc.) microbeads,[80] which, however, could not form tight organizations[81] due to the high stiffness and lack of binding points of these hydrogels. Therefore, the droplet culturing method[82] and the core-shell method,[83] such as (liquid core, collagen core, etc.), were widely investigated. As for organoids, the manipulation of the matrix (such as Matrigel and BME2) on the chip is challenging due to their tens-of-minutes solidification. As shown in Figure 5B, pure Matrigel droplets were generated on the flow-focusing chip under 4 °C, followed by 37 °C incubation for half an hour. The Matrigel microbeads can be stored in the organoid medium for a few weeks, which meets
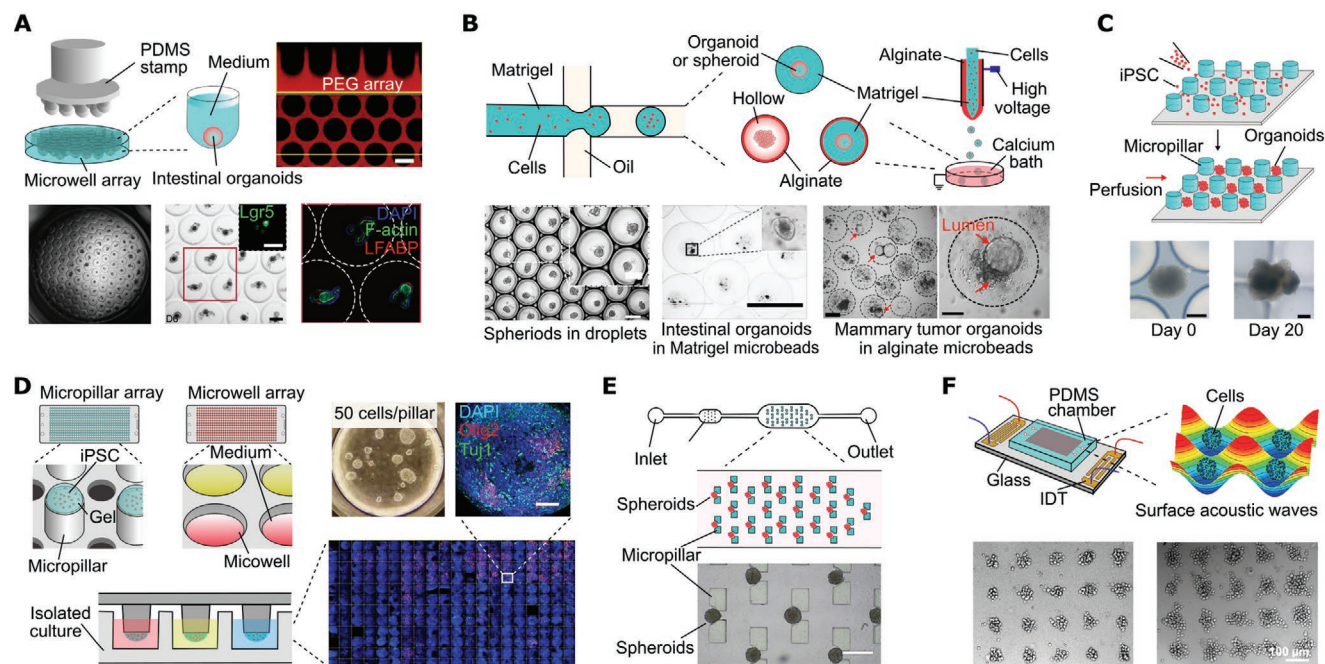

Figure 5. High-throughput generation and analysis on microfluidic chips. A) Microwell-based development of gastrointestinal organoids with suspension culture. Scale bar: 200 μm. Reproduced with permission.[77] Copyright 2020, Nature Publishing Group. B) Droplet technique for the massive culture of spheroids and organoids. Pure hydrogel microbeads, hollow microbeads, and microbeads with Matrigel core and alginate shell were generated for different kinds of spheroids and organoids. Scale bar: 500 and 200 μm (left), 2 mm (right). Reproduced with permission.[62,82a,85] Copyright 2018, Elsevier; 2017 and 2021, Wiley-VCH GmbH. C) Liver organoids developed among the micropillars. Scale bar: 50 μm. Reproduced with permission.[89] Copyright 2018, Royal Society of Chemistry. D) High-throughput micropillar-microwell array for the independent culture of PSCs. Scale bar: 1 mm. Reproduced with permission.[90] Copyright 2020, the American Association for the Advancement of Science. E) Intestinal enteroids captured by the micropillars for in situ observation. Reproduced with permission.[91] Copyright 2014, AIP Publishing Group. F) High-throughput generation of spheroids via the surface acrostic wave techniques. Scale bar: 100 μm. Reproduced with permission.[93] Copyright 2016 and 2019, Royal Society of Chemistry.

**ADVANCED
SCIENCE NEWS**

www.advancedsciencenews.com

**ADVANCED
FUNCTIONAL
MATERIALS**

www.afm-journal.de

the requirement of acinar organoids.[84] To enhance the solidification and strength, the Matrigel microbeads were optimized with an alginate shell by electrostatic co-spraying technique. Due to the enhanced mass transfer in droplets, the gastrointestinal organoids had higher expression of CD44, Lgr5 and Ki67 than in bulk culture.[85] An interesting finding is that the mouse mammary tumor organoids can be established in nonadhesive alginate by embedding the tumor pieces inside. Thus, it is easy to achieve the high-throughput generation of mammary tumor organoids in pure alginate microbeads.[62] Some organoids (islet organoids, etc.) that do not need the support of the matrix can be scaled up in microbeads with liquid core and alginate shell.[86] Moreover, the hydrogel fibre similarly generated on the chip can also be used for high-throughput analysis of spheroids and organoids.[87]

2.3.3. Micropillars

Micropillars on the chip can also work well in the high-throughput development of spheroids and organoids. One function of these micropillars is the spatial separation and cell gathering into small groups.[88] As shown in Figure 5C, the iPSCs seeded among the micropillars aggregated together and then differentiated into the liver organoids under the perfusion of the differentiation medium.[89] Integrated with the microwell array, the micropillar array can achieve high-throughput screen of dosage, duration dynamics and combinations of cellular factors. As shown in Figure 5D, the gel-encapsulated human iPSC cells seeded on the top of each micropillar were then inserted inside the microwells for independent culture. The microengineering vastly enhanced the capacity of throughput compared to the 96-well or 386-well plates.[90] As shown in Figure 5E, the PDMS micropillars in the microfluidic chamber were used to capture the mouse intestinal enteroids. The volume change could be observed in situ.[91] Parameters such as the size, shape, and density of the micropillars were critical for this design.

2.3.4. Surface Acoustic Wave

The surface acoustic wave technique has been widely used in microfluidics for cell arrangement,[92] which could help for the high-throughput generation of spheroids. As shown in Figure 5F, the interdigital transducers are usually integrated into the chip, which generates the acrostic field in the cell-suspended chamber. The HepG2 cells would move to the pressure node and form small clusters, which then grow into spheroids.[93] It should be noticed that the surface acoustic wave chip also showed great potentials in precision manipulation, such as guiding the organoids fusion in high throughput and low variability.[94]

2.4. Co-Culture and Multi-Tissue Interactions

The microenvironment of cells in vivo involves interactions with other cells (stroma cells, immune cells, etc.) and tissues or organs. The complexity works together to maintain homeostasis

and functions. Spheroids- and organoids-on-a-chip technology facilitates the investigation of the co-culture and multi-tissue interactions due to the easy control, integration, and analysis on the chip.

2.4.1. Co-Culture with HUVECs for Vascularization

One issue of in vitro spheroids and organoids is the limited nutrition supply with the increased size due to the lack of a vascular network.[95] Therefore, establishing a vascular network in these models has great significance.[96] Some studies show that the microfluidic channels can mimic blood vessels to some extent.[89,97] However, this is not the natural solution and lacks essential interactions. The epithelial blood vessels have been successfully generated on the chip through vasculogenesis or angiogenesis.[98] The strategy for spheroid vascularization is to co-culture the spheroid with the established blood vessel network. As shown in **Figure 6**A, human umbilical vein endothelial cells (HUVECs) can be seeded on the lateral channels. The middle channel was filled with hydrogel (usually the fibrinogen), which suited the blood vessel formation. The MCF-7 breast tumor spheroids were loaded inside the middle channel. After several days of co-culture, the vascular network could merge with the spheroids, as shown in the side view. Fluorescent flowing experiments showed the vascular network could facilitate transportation, allowing higher proliferation activities and lower cell death. It should be noted that the normal human lung fibroblasts could accelerate vascularization in the co-culture system due to their continuous paracrine signals.[99]

There are two strategies for the vascularization of organoids. One is directly mixing the HUVECs with the organoid cells[100] or co-differentiation with mesodermal progenitors.[101] For instance, kidney organoids' vascularization co-differentiated the stem cells into pretubular aggregates and kidney organoids.[43] Here we detailly discuss another strategy similar to the above vascularization of spheroids. Taking the colon organoids as an example, the challenge is the optimizing ECM and culturing medium for both blood vessels and colon organoids, as shown in Figure 6B. In the conventional culture, the ECM for blood vessels is the fibrinogen and that for colon organoids is the Matrigel; the medium for the former and the latter is the endothelial growth medium (ECGM2) and colon organoids medium, respectively. Shravanthi et al. investigated various conditions and finally confirmed the optimal parameters are 50% ECGM2 and 50% colon medium, 90% fibrin and 10% v/v Matrigel for the final ECM. The plate changed the tilt every 15 mins. Under these conditions, the colon organoids could merge well with the vascular network.[102] The vascularization of organoids is the basis in transplant in vivo[103] and drug delivery.[104]

2.4.2. Co-Culture with Immune Cells

Tumor-immune interactions in the tumor microenvironment govern the tumor progression and drug response. The spheroids- and organoids-on-a-chip technology becomes an excellent tool to investigate these interactions due to the
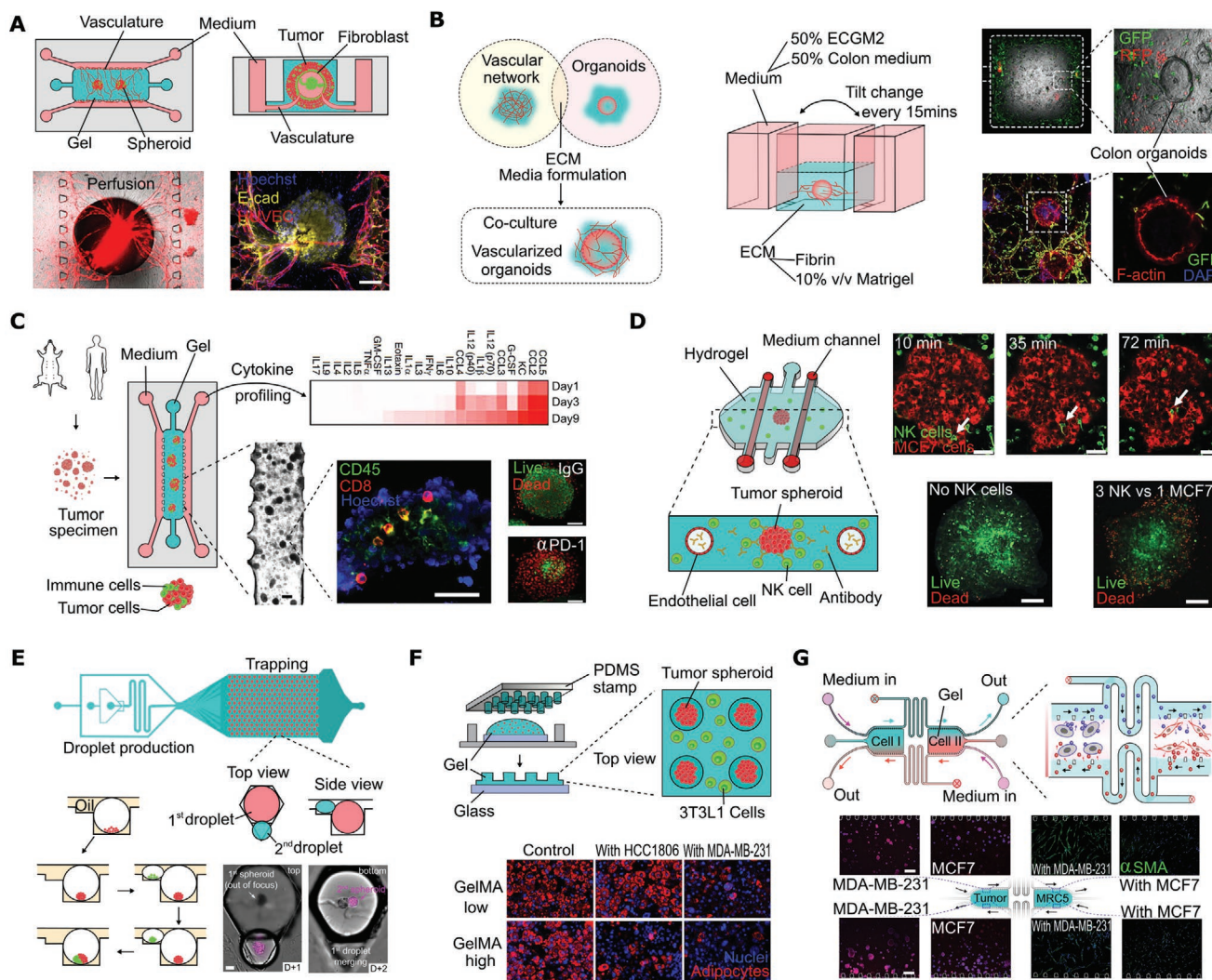
Figure 6. Co-culture and multi-tissue interactions on the chip. A) Vascularization of tumor spheroids on the chip with the vascular network. Scale bar: 50 μm. Reproduced with permission.[99a] Copyright 2020, Elsevier. B) Vascularization of colon organoids with the vascular network. Reproduced with permission.[102] Copyright 2020, Wiley-VCH GmbH. C) Immune checkpoint blockade therapy demonstrated on the tumor spheroids on a chip can achieve tumor microenvironment maintenance, histological analysis, cytokine profiling, live/dead imaging and drug screening. Scale bar: 0.5 mm (left), 50 μm (middle and right). Reproduced with permission.[106a] Copyright 2018, AACR publications. D) Dynamic targeting tumor spheroids by NK cells migrating through blood vessels and dense cells on the chip. Scale bar: 50 μm (top) and 200 μm (bottom). Reproduced with permission.[108] Copyright 2019, Taylor & Francis Group. E) Spheroid sequential merging on the anchors chip for various types of co-culture. Scale bar: 50 μm. Reproduced with permission.[109] Copyright 2020, Elsevier. F) Stamp-based microfluidic chip for the co-culture of tumor spheroids and adipocytes. Reproduced with permission.[110] Copyright 2018, Elsevier. G) Unidirectional intercellular communication on the chip. Scale bar: 200 μm. Reproduced with permission.[20a] Copyright 2020, Elsevier.

convenient observation, cell manipulation and sample analysis.[105] Immune checkpoint blockade has been demonstrated as an effective tumor clinical therapy. However, inevitably, the monoclonal antibody (e.g., PD-1 and CTLA4) targeting therapy suffers from significant toxicity for some patients. Precision immune-tumor in vitro trials are essential, which require the analysis of immune-tumor interactions on the chip. As shown in Figure 6C, the CT26 tumor spheroids derived from murine were seeded on the chip, which contained the autologous lymphoid and myeloid cells. After 6 days of culture, the spheroids can flourish while maintaining the immune cells. Cytokines can be profiled by sampling on the chip. The control experiments of αPD-1 and IgG illustrated the sensitivity of tumor

response to immune checkpoint blockade therapy.[106] Another example is that a similar microfluidic model was established for hepatitis B virus-related hepatocellular carcinoma.[107]

In immunotherapy, the immune cells need to extravasate through the blood vessel and target the tumor by migrating through the dense cells. This dynamic progress is hard to be investigated in conventional in vitro models. The on-chip technology facilitates the study of these dynamic processes. As shown in Figure 6D, a microfluidic chip was designed to study the natural killer (NK) cells targeting the breast tumor spheroids. Artificial blood vessels were established, and the NK cells' activity could be real-time monitored on the chip. Results indicated that the NK cells could sense the presence of tumor

spheroid several hundred micrometers away and kill tumor cells from both the periphery and innermost layers.[108]

2.4.3. Co-Culture with Stromal Cells

The co-culture of spheroids/organoids with other stromal cells is widely investigated on the chip, such as the fibroblasts, cancer-associated fibroblasts (CAFs), stellate cells, and adipocytes.[87b,104a,111] Strategies such as on-chip spatial arranging and multicompartment microbeads and fibres are chosen for the investigation. More recently, some versatile and innovative methods have been developed. As shown in Figure 6E, a strategy for spheroid sequential merging was presented using the droplet-capillary anchors. The step-like anchors allowed the capture of droplets sequentially where spheroids were developed. By triggering the droplet merger, different kinds of spheroids could grow together in a single droplet. This cascaded culture allows the dynamic control of cell-cell interactions and the heterogeneity of 3D culture.[109] As shown in Figure 6F, a stamp-based microfluidic chip was used to investigate the interactions of breast tumor spheroids (in the wells) and adipocytes (on the surface). It indicates the differentiation to adipocytes was decreased significantly by the tumor cells.[110] A similar design is utilized for co-culture gut organoids and epithelial cells/fibroblasts.[112] In conventional co-culture, the signal molecules secreted from different types of cells diffuse randomly, hiding the intrinsic phenomenon. As shown in Figure 6G, the unidirectional communication of cells was designed on the chip. The medium flowed oppositely in the lateral channels controlled by the syringe pump, delivering the signals directionally. In the chamber, the cells on the top were affected, and the cells at the bottom could avoid the influence. Differentiation from normal fibroblasts to CAFs induced by breast tumor spheroids was investigated on this chip.[20a]

2.5. Biosensing and Bioimaging Integration

To date, most of the applications of spheroids and organoids are still stuck in the laboratory, limited by the lack of generalized and standardized analyzing methods and evaluation criteria. Manual manipulation and judgment involve huge errors. The spheroids- and organoids-on-a-chip technology enables the integration of biosensing and bioimaging, allowing automatic analysis and decreased error.

2.5.1. Electrochemical Sensor

Electrochemical sensors have been widely used for the monitoring of biochemical parameters, such as pH,[113] oxygen,[114] and glucose.[115] As shown in **Figure 7**A, a representative setup is designed to continuously monitor the lactate and glucose secreted by on-chip human colon tumor spheroids. The electrode chip could be plugged into the hanging-drop chip, which contains four platinum working electrodes (WE), a platinum counter electrode (CE) and an Ag/AgCl reference electrode (RE). To monitor the lactate and the glucose, the electrode was functionalized with the oxidase enzymes.[116] Except for these general parameters, other specific biomarkers are required to be monitored. Common methods, such as immunosorbent assays (ELISA) and surface plasma resonance (SPR), sometimes suffer limited sensitivity and nonspecific binding.[117] To increase the sensitivity and selectivity, for instance, the aptamer-functionalized electrode was designed to capture the creatine kinase-MB (biomarkers secreted by the damaged cardiac organoids), as shown in Figure 7B.[118]

Cardiac spheroids and organoids are attractive and critical 3D models which usually require the measurement of dynamic electronic signals, beat rhythm and contraction force. Various methods are developed, such as printed electrodes,[119] flexible electrodes,[120] nanoelectronics mesh,[121] and electronical nanopillars.[122] As shown in Figure 7C, a self-rolled biosensor array was used to multiplex record the field potentials on the surface of the cardiac spheroids, even the calcium imaging. This strategy allowed high sensitivity and spatiotemporal resolution.[123] Except for the measurement of the electronical signal, the influence of the electric field on the spheroids can also be investigated on the chip.[124] The neural activities of spinal organoids could be recorded via the on-chip electrode array.[125]

2.5.2. On-Chip Imaging

Another advance of the spheroids- and organoids-on-a-chip technology is the easy integration of bioimaging. Good-quality imaging requires high resolution, large field of view (FoV), strong penetration, and high speed. Spheroids and organoids on the chip usually limit the light penetration and show significant light scattering due to their high cell density and large size. As shown in Figure 7D, the on-chip clearing technique for 3D tissues (breast tumor spheroids) was described. Different processing can be sequentially introduced into the channels. The scattering lipid molecules that hind the imaging can be removed fast by 567-folds, allowing the 20× faster than the current passive clearing approaches.[126]

FoV of conventional imaging, such as the commonly-used confocal microscopy, is limited by the numerical aperture of the objective lens, which impedes the advances of spheroids- and organoids-on-a-chip technology. Lens-free imaging promises large FoV and high resolutions,[127] especially suiting the integration with microfluidic chips.[128] As shown in Figure 7E, a lens-free imaging system was integrated with the spheroids on a chip. The setup generally contains multi-angle or multi-color light sources, imaging sensors (CMOS or CCD) and the sample chip. Light propagates through the samples and arrives on the image sensors with the phase information. Results illustrated the achieved image could be as good as confocal microscopy. The FoV could reach 3.4 mm × 2.3 mm × 0.3 mm.[129] Another potential imaging method for the spheroids- and organoids-on-a-chip technology is the chip-based nanoscopy, which ensures large FoV and super-resolution. This mainly relies on the high-integrated and high-refractive-index waveguide chip, combined with structured illumination microscopy (SIM)[130] or stochastic optical reconstruction microscopy (STORM).[131] As shown in Figure 7F, the high-refractive-index waveguide chip could provide strong evanescent light for fluorescent molecule
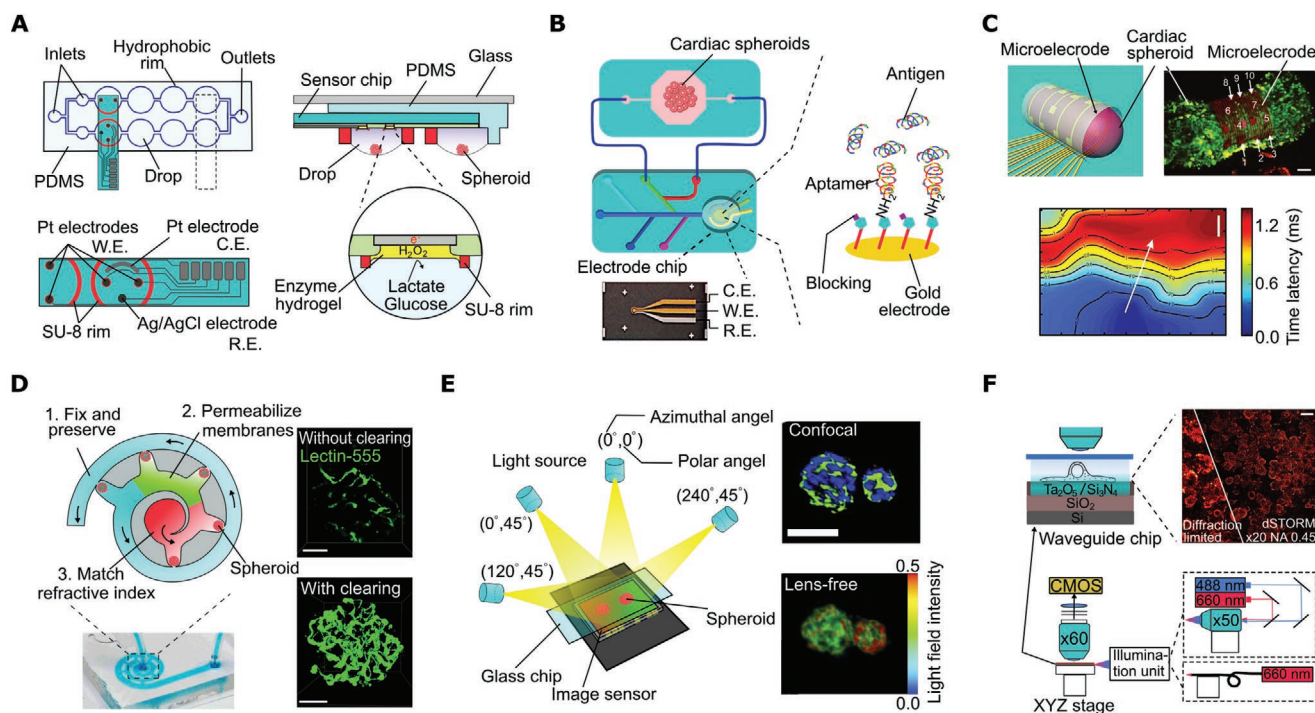
Figure 7. Integration of biosensing and bioimaging with spheroids- and organoids-on-a-chip technology. A) Continuous monitor the lactate and glucose by electrochemical sensors integrated with the spheroids on a chip. Reproduced with permission.[116] Copyright 2016, Nature Publishing Group. B) Aptamer-functionalized electrode for detecting creatine kinase-MB with the cardiac organoids on a chip. Reproduced with permission.[118] Copyright 2016, American Chemical Society. C) Self-rolled biosensor array for the recording of the potential field of cardiac spheroids. Scale bar: 50 μm. Reproduced with permission.[123] Copyright 2019, the American Association for the Advancement of Science. D) On-chip clearing of spheroids, which is 20× faster than the conventional clearing approach. Scale bar: 50 μm. Reproduced with permission.[126] Copyright 2017, the National Academy of Science. E) Lens-free imaging for the spheroids on a chip. Scale bar: 50 μm. Reproduced with permission.[129] Copyright 2020, OSA publishing. F) On-chip STORM-based wide FoV nanoscopy. Scale bar: 50 μm. Reproduced with permission.[131] Copyright 2017, Nature Publishing Group.

switching. The STORM on-chip microscopy ensures an FoV of 0.5 mm × 0.5 mm and a resolution of ≈340 nm. It is also believed that lattice light-sheet microscopy could have good applications for on-chip high-throughput analysis.[132] Imaging for the deep penetration of spheroids and organoids was also investigated.[133]

3. Future Perspective

With the fast development of spheroids- and organoids-on-a-chip technology, we envision three future directions in this field, as shown in **Figure 8**. First, the complexity and systematicness will be highly increased on the chip. The high complexity of the microenvironment synergizes to allow homeostasis in vivo. The spheroids- and organoids-on-a-chip technology that can furthest replicate the microenvironment should consist of the vascular network, immune cells, and other stromal cells (fibroblasts, mesenchymal stroma cells, etc.), mechanical stimulus, and even the symbiotic microbiota for the specific microenvironment (stomach or intestine).[134] Miniatured multi-functional sensors offer critical parameters of the microenvironment.[135] Specific spheroids or organoids such as the cardiac or gastrointestinal area require related mechanical stimulus. Simultaneously, conventional spherical morphology may be replaced by organ-like large-scale architecture guided by spatial control.

Second, a fast and concise strategy for the body-on-a-chip system could be offered via the spheroids and organoids on a chip. The complicated functions and activities in the human body rely on signaling pathways and hormonal stimulating loops among various organs, which promise homeostasis. One important application of the spheroid/organoid models is drug screening, which usually involves the quantification of pharmacokinetics and predictions of ADME (absorption, distribution, metabolism, and excretion). However, this mainly requires cross-organ analysis, which is still challenging for in vivo animal models because of high cost, ethical concerns, and differences in genetic background.

Body-on-a-chip technology mimics the intrinsic interactions among the organs and further offers the ADME of the drug trials in each organ. Organ-on-a-chip technology could well constitute the body on a chip, which has achieved the robotic assemblage.[136] For instance, the most common combination of the liver and other organs (such as the heart, lung, and kidney) could provide hepatotoxicity and molecule metabolites during drug trials.[137] The combination of vasculature and brain on the chip could mimic the blood-brain barrier.[138]

Combining various spheroids and organoids into a single chip to mimic the body is more convenient and avoids the complex chip manufacturing in the organ-on-a-chip system.[139] For instance, a tripartite culture system was made by assembling the liver, stomach and intestinal organoids into a single
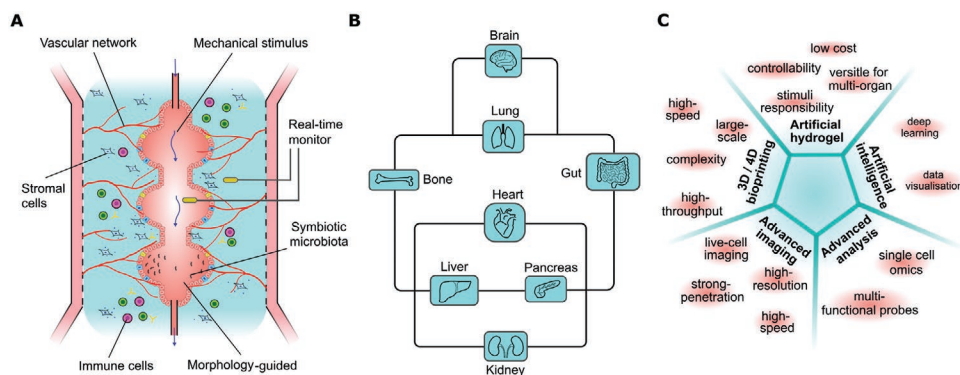
Figure 8. Future perspective of the spheroids- and organoids-on-a-chip technology. A) Higher complexity and systematicness integrated with heterogeneous cells, vascular network, mechanical stimulus, symbiotic microbiota, monitoring sensors, and guided morphology. B) Human body-on-a-chip for advanced disease modelling and drug screening. C) Combination with other advanced emerging technology.

microwell chip.[100a] The design suited high-throughput analysis and involved dynamic culture easily. The bile acid-induced regulation of the enzyme CYP7A1 in hepatic tissue by the intestinal organoids was investigated. It indicates that the high level of chenodeoxycholic acid resulted in lower expression of CYP7A1 expression in hepatic tissue, likely due to the secretion of paracrine factors (e.g., FGF-15) from the intestinal organoid. Mimicking the Transwell platforms, Fangchao Yin et al. designed the liver-heart organoids- on-chip device for the assessment of the cardiac safety of an antidepressant drug, following liver metabolism in vitro.[139] Therefore, compared to the organ-on-chip technology, the body-on-chip technology based on spheroids and organoids can facilitate the high-throughput integration and separated organoid-level analysis, which can primarily benefit the large-scale evaluation in drug screening.

Obviously, there still remain significant challenges in the body-on-a-chip system. One issue for the multi-organoids on a chip is the medium, as each type of organoid requires different composition of the medium. Different medium is even needed for the different states of single-type organoids. How to optimize the medium for the whole system is still seldom explored. Another issue is how to adjust the number, size, and even the age of each organoid to reach an appropriate scaling for the whole constitution as the difference in scaling may cause various growth and communication of the organoids.[140]

Expensive EHS mouse tumor derived Matrigel limits the promotion and industrialization of organoid technology. New artificial hydrogels are in urgent demand and require low cost, high controllability, good versatility for multi-organs, and suitable stimuli responsibility. To date, PEG-based functional hydrogels have been used preliminarily.[68,141]

PDMS-based devices remain prodigious as their excellent beneficial properties, such as high elasticity, low cost, easy operation in soft lithography, good optical transparency, good oxygen penetration, and biocompatibility. However, it is also reported that PDMS can absorb small hydrophobic molecules, which potentially affect cell signaling and drug screening efficiency.[142] Therefore, some devices based on other alternative materials are proposed, such as glass,[143] silicon,[144] thermoplastics,[145] paper,[146] hydrogels,[147] ceramics, etc. Glass and silicon hold great pressure resistance, chemical stability, and

optical transparency. The established semiconductor technology can be applied for batch fabrication. Thermoplastic polymers, such as polystyrene, poly(lactic acid) (PLA) and poly(methyl methacrylate) (PMMA), have low cost, high biocompatibility, and good mechanical strength, but lack permeability and flexibility. Paper-based devices are flexible, highly porous, easily modified and biocompatible, but have limitations in transparency and mechanical strength when getting wet.[148] With the help of stereolithography and 3D bioprinting, hydrogels (such as PEGDA and ECM-based hydrogels) can be directly fabricated into the devices, which promises good perfusion and high similarity to native tissues.[149] Bio-ceramics show bright potential applications in mimicking the microenvironment of bone marrow due to the highly porous and suitable mechanical structures.[150] Overall, the request of materials in device fabrication should be considered in terms of cost, fabrication method, biocompatibility, mechanical features, oxygen permeability, optical clarity, and molecule absorption.

The emerging 3D and 4D bioprinting technologies allow more complex and large-scale models in cell arrangement, biomaterials control, morphology guidance, and batch production.[26,151] Artificial intelligence, represented by machine learning, enables high-efficiency analysis in drug discovery, bio-sample recognition, and classification.[152] Integrated with microfluidic technology (e.g., droplet technique), it could simplify biotechnology research and enhance logical analysis and prediction.[153] Advanced imaging technology, such as lattice light-sheet microscopy, super-resolution microscopy, expansion microscopy, and on-chip imaging technique, would give insight into cellular progress on a nanoscale.[154] Advanced analysing technologies are also required in this field, such as single-cell omics and multi-functional probes.[155]

2215043 (13 of 19)

**ADVANCED
SCIENCE NEWS**

www.advancedsciencenews.com

**ADVANCED
FUNCTIONAL
MATERIALS**

www.afm-journal.de

Conflict of Interest

The authors declare no conflict of interest.

Keywords

3D cellular models, cellular microenvironments, microfluidics, organoid on a chip, spheroid on a chip

[1] B. M. Baker, C. S. Chen, *J. Cell Sci.* **2012**, *125*, 3015.

[2] M. Kapalczynska, T. Kolenda, W. Przybyla, M. Zajaczkowska, A. Teresiak, V. Filas, M. Ibbs, R. Blizniak, L. Luczewski, K. Lamperska, *Arch. Med. Sci.* **2018**, *14*, 910.

[3] Global 3D Cell Culture Market, https://www.strategicmarketresearch.com/market-report/3d-cell-culture-market (accessed: May 2022).

[4] F. Hirschhaeuser, H. Menne, C. Dittfeld, J. West, W. Mueller-Klieser, L. A. Kunz-Schughart, *J. Biotechnol.* **2010**, *148*, 3.

[5] R. Z. Lin, H. Y. Chang, *Biotechnol. J.* **2008**, *3*, 1172.

[6] a) K. Moshksayan, N. Kashaninejad, M. E. Warkiani, J. G. Lock, H. Moghadas, B. Firoozabadi, M. S. Saidi, N.-T. Nguyen, *Sens. Actuators, B* **2018**, *263*, 151; b) H.-W. Han, S. Asano, S.-h. Hsu, *Appl. Sci.* **2019**, *9*, 627; c) X. Cui, Y. Hartanto, H. Zhang, *J R Soc Interface* **2017**, *14*, 20160877.

[7] a) S. M. Weis, D. A. Cheresh, *Nat. Med.* **2011**, *17*, 1359; b) F. Virga, M. Ehling, M. Mazzone, *Cell Metab.* **2019**, *30*, 16.

[8] a) M. Azharuddin, K. Roberg, A. K. Dhara, M. V. Jain, P. Darcy, J. Hinkula, N. K. H. Slater, H. K. Patra, *Sci. Rep.* **2019**, *9*, 20066; b) R. Barrera-Rodriguez, J. M. Fuentes, *Cancer Cell Int.* **2015**, *15*, 47.

[9] a) J. M. Santos, S. P. Camoes, E. Filipe, M. Cipriano, R. N. Barcia, M. Filipe, M. Teixeira, S. Simoes, M. Gaspar, D. Mosqueira, D. S. Nascimento, O. P. Pinto-do, C. Pruz, H. Cruz, M. Castro, J. P. Miranda, *Stem Cell Res Ther* **2015**, *6*, 90; b) Y. Li, E. Kumacheva, *Sci. Adv.* **2018**, *4*, eaas8998.

[10] H. Clevers, *Cell* **2016**, *165*, 1586.

[11] M. Simian, M. J. Bissell, *J. Cell Biol.* **2017**, *216*, 31.

[12] N. Picollet-D'hahan, M. E. Dolega, D. Freida, D. K. Martin, X. Gidrol, *Trends Biotechnol.* **2017**, *35*, 1035.

[13] Z. Wang, X. He, H. Qiao, P. Chen, *Tissue Eng Part A* **2020**, *26*, 656.

[14] G. Saorin, I. Caligiuri, F. Rizzolio, *Semin Cell Dev Biol* **2022**, *10*, 1.

[15] a) Y. Wu, Y. Zhou, X. Qin, Y. Liu, *Biomicrofluidics* **2021**, *15*, 061503; b) V. S. Shirure, C. C. W. Hughes, S. C. George, *Annu. Rev. Biomed. Eng.* **2021**, *23*, 141.

[16] Y. Wang, M. Liu, Y. Zhang, H. Liu, L. Han, *Lab Chip* **2023**.

[17] a) A. Manfrin, Y. Tabata, E. R. Paquet, A. R. Vuaridel, F. R. Rivest, F. Naef, M. P. Lutolf, *Nat. Methods* **2019**, *16*, 640; b) G. S. Lim, J. H. Hor, N. R. Y. Ho, C. Y. Wong, S. Y. Ng, B. S. Soh, H. Shao, *Theranostics* **2019**, *9*, 311.

[18] M. R. Carvalho, D. Barata, L. M. Teixeira, S. Giselbrecht, R. L. Reis, J. M. Oliveira, R. Truckenmüller, P. Habibovic, *Sci. Adv.* **2019**, *5*, eaaw1317.

[19] P. Rifes, M. Isaksson, G. S. Rathore, P. Aldrin-Kirk, O. K. Moller, G. Barzaghi, J. Lee, K. L. Egerod, D. M. Rausch, M. Parmar, T. H. Pers, T. Laurell, A. Kirkeby, *Nat. Biotechnol.* **2020**, *38*, 1265.

[20] a) G. Fang, H. Lu, H. Aboulkheyr Es, D. Wang, Y. Liu, M. E. Warkiani, G. Lin, D. Jin, *Biosens. Bioelectron.* **2021**, *175*, 112833; b) D. Ellison, A. Mugler, M. D. Brennan, S. H. Lee, R. J. Huebner, E. R. Shamir, L. A. Woo, J. Kim, P. Amar, I. Nemenman, A. J. Ewald, A. Levchenko, *Proc Natl Acad Sci U S A* **2016**, *113*, E679; c) S. Cosson, M. P. Lutolf, *Sci. Rep.* **2014**, *4*, 4462.

[21] a) W. Lim, S. Park, *Molecules* **2018**, *23*, 3355; b) T. Mulholland, M. McAllister, S. Patek, D. Flint, M. Underwood, A. Sim, J. Edwards, M. Zagnoni, *Sci. Rep.* **2018**, *8*, 14672; c) O. Frey, P. M. Misun, D. A. Fluri, J. G. Hengstler, A. Hierlemann, *Nat. Commun.* **2014**, *5*, 4250.

[22] Z. Zhang, Y. C. Chen, S. Urs, L. Chen, D. M. Simeone, E. Yoon, *Small* **2018**, *14*, 1703617.

[23] a) B. Schuster, M. Junkin, S. S. Kashaf, I. Romero-Calvo, K. Kirby, J. Matthews, C. R. Weber, A. Rzhetsky, K. P. White, S. Tay, *Nat. Commun.* **2020**, *11*, 5271; b) J. Tischler, Z. Swank, H. A. Hsiung, S. Vianello, M. P. Lutolf, S. J. Maerkl, *Cell Rep Methods* **2022**, *2*, 100244.

[24] D. Baptista, L. M. Teixeira, Z. T. Birgani, S. van Riet, T. Pasman, A. Poot, D. Stamatialis, R. J. Rottier, P. S. Hiemstra, P. Habibovic, C. van Blitterswijk, S. Giselbrecht, R. Truckenmuller, *Biomaterials* **2021**, *266*, 120436.

[25] a) M. Nikolaev, O. Mitrofanova, N. Broguiere, S. Geraldo, D. Dutta, Y. Tabata, B. Elci, N. Brandenberg, I. Kolotuev, N. Gjorevski, H. Clevers, M. P. Lutolf, *Nature* **2020**, *585*, 574; b) N. Gjorevski, M. Nikolaev, T. E. Brown, O. Mitrofanova, N. Brandenberg, F. W. DelRio, F. M. Yavitt, P. Liberali, K. S. Anseth, M. P. Lutolf, *Science* **2022**, *375*, eaaw9021.

[26] J. A. Brassard, M. Nikolaev, T. Hubscher, M. Hofer, M. P. Lutolf, *Nat. Mater.* **2021**, *20*, 22.

[27] Z. Ao, H. Cai, Z. Wu, S. Song, H. Karahan, B. Kim, H. C. Lu, J. Kim, K. Mackie, F. Guo, *Lab Chip* **2021**, *21*, 2751.

[28] Y. Liu, C. Dabrowska, A. Mavousian, B. Strauss, F. Meng, C. Mazzaglia, K. Ouaras, C. Macintosh, E. Terentjev, J. H. Lee, Y. Y. S. Huang, *Adv. Sci. (Weinh)* **2021**, *8*, 2003332.

[29] T. Sato, H. Clevers, *Science* **2013**, *340*, 1190.

[30] a) Y. Wang, D. B. Gunasekara, M. I. Reed, M. DiSalvo, S. J. Bultman, C. E. Sims, S. T. Magness, N. L. Allbritton, *Biomaterials* **2017**, *128*, 44; b) Y. Wang, R. Kim, D. B. Gunasekara, M. I. Reed, M. DiSalvo, D. L. Nguyen, S. J. Bultman, C. E. Sims, S. T. Magness, N. L. Allbritton, *Cell Mol. Gastroenterol. Hepatol.* **2018**, *5*, 113.

[31] J. Creff, R. Courson, T. Mangeat, J. Foncy, S. Souleille, C. Thibault, A. Besson, L. Malaquin, *Biomaterials* **2019**, *221*, 119404.

[32] a) Z. Ma, J. Wang, P. Loskill, N. Huebsch, S. Koo, F. L. Svedlund, N. C. Marks, E. W. Hua, C. P. Grigoropoulos, B. R. Conklin, K. E. Healy, *Nat. Commun.* **2015**, *6*, 7413; b) P. Hoang, J. Wang, B. R. Conklin, K. E. Healy, Z. Ma, *Nat. Protoc.* **2018**, *13*, 723.

[33] M. Bosch-Fortea, A. E. Rodriguez-Fraticelli, G. Herranz, M. Hachimi, M. D. Barea, J. Young, B. Ladoux, F. Martin-Belmonte, *Biomaterials* **2019**, *218*, 119339.

[34] J. Kim, Y. Zheng, A. A. Alobaidi, H. Nan, J. Tian, Y. Jiao, B. Sun, *Biophys. J.* **2020**, *118*, 1177.

[35] S. Wei, L. Hongxu, N. Kawazoe, C. Guoping, *Journal of Bioactive and Compatible Polymers* **2011**, *26*, 242.

[36] E. Wang, D. Wang, A. Geng, R. Seo, X. Gong, *Biomaterials* **2017**, *143*, 57.

[37] G. Fang, H. Lu, A. Law, D. Gallego-Ortega, D. Jin, G. Lin, *Lab Chip* **2019**, *19*, 4093.

[38] a) M. Marimuthu, N. Rousset, A. St-Georges-Robillard, M. A. Lateef, M. Ferland, A. M. Mes-Masson, T. Gervais, *Lab Chip*

2018, *18*, 304; b) W. Liu, M. Sun, B. Lu, M. Yan, K. Han, J. Wang, *Sens. Actuators, B* **2019**, *292*, 111.

[39] A. Pasturel, P. O. Strale, V. Studer, *Adv. Healthcare Mater.* **2020**, *9*, 2000519.

[40] a) Y. Ma, M. Lin, G. Huang, Y. Li, S. Wang, G. Bai, T. J. Lu, F. Xu, *Adv. Mater.* **2018**, *30*, 1705911; b) P. Romani, L. Valcarcel-Jimenez, C. Frezza, S. Dupont, *Nat. Rev. Mol. Cell Biol.* **2021**, *22*, 22; c) K. H. Vining, D. J. Mooney, *Nat. Rev. Mol. Cell Biol.* **2017**, *18*, 728.

[41] a) O. O. Arishe, A. B. Ebeigbe, R. C. Webb, *Am. J. Hypertens.* **2020**, *33*, 1; b) J. Li, B. Hou, S. Tumova, K. Muraki, A. Bruns, M. J. Ludlow, A. Sedo, A. J. Hyman, L. McKeown, R. S. Young, N. Y. Yuldasheva, Y. Majeed, L. A. Wilson, B. Rode, M. A. Bailey, H. R. Kim, Z. Fu, D. A. Carter, J. Bilton, H. Imrie, P. Ajuh, T. N. Dear, R. M. Cubbon, M. T. Kearney, R. K. Prasad, P. C. Evans, J. F. Ainscough, D. J. Beech, *Nature* **2014**, *515*, 279.

[42] a) A. Marturano-Kruik, M. M. Nava, K. Yeager, A. Chramiec, L. Hao, S. Robinson, E. Guo, M. T. Raimondi, G. Vunjak-Novakovic, *Proc Natl Acad Sci U S A* **2018**, *115*, 1256; b) K. Rennert, S. Steinborn, M. Groger, B. Ungerbock, A. M. Jank, J. Ehgartner, S. Nietzsche, J. Dinger, M. Kiehntopf, H. Funke, F. T. Peters, A. Lupp, C. Gartner, T. Mayr, M. Bauer, O. Huber, A. S. Mosig, *Biomaterials* **2015**, *71*, 119; c) T. M. Ken Hiratsuka, Katharina T. Kroll, Navin R. Gupta, M. Todd Valerius, Thomas Ferrante, Michifumi Yamashita, Jennifer A. Lewis, Ryuji Morizane, *Sci. Adv.* **2022**, *8*, eabq0866; d) Y. Xue, M. J. Seiler, W. C. Tang, J. Y. Wang, J. Delgado, B. T. McLelland, G. Nistor, H. S. Keirstead, A. W. Browne, *Lab Chip* **2021**, *21*, 3361.

[43] K. A. Homan, N. Gupta, K. T. Kroll, D. B. Kolesky, M. Skylar-Scott, T. Miyoshi, D. Mau, M. T. Valerius, T. Ferrante, J. V. Bonventre, J. A. Lewis, R. Morizane, *Nat. Methods* **2019**, *16*, 255.

[44] J. L. Yesl Jun, Seongkyun Choi, Ji Hun Yang, Maike Sander, S. Chung, S.-H. Lee, *Sci. Adv.* **2019**, *5*, eaax4520.

[45] K. K. Lee, H. A. McCauley, T. R. Broda, M. J. Kofron, J. M. Wells, C. I. Hong, *Lab Chip* **2018**, *18*, 3079.

[46] H. B. Chong, J. Youn, W. Shin, H. J. Kim, D. S. Kim, *Lab Chip* **2021**, *21*, 3316.

[47] E. Berger, C. Magliaro, N. Paczia, A. S. Monzel, P. Antony, C. L. Linser, S. Bolognin, A. Ahluwalia, J. C. Schwamborn, *Lab Chip* **2018**, *18*, 3172.

[48] X. Qian, H. N. Nguyen, M. M. Song, C. Hadiono, S. C. Ogden, C. Hammack, B. Yao, G. R. Hamersky, F. Jacob, C. Zhong, K. J. Yoon, W. Jeang, L. Lin, Y. Li, J. Thakor, D. A. Berg, C. Zhang, E. Kang, M. Chickering, D. Nauen, C. Y. Ho, Z. Wen, K. M. Christian, P. Y. Shi, B. J. Maher, H. Wu, P. Jin, H. Tang, H. Song, G. L. Ming, *Cell* **2016**, *165*, 1238.

[49] H. Cai, Z. Ao, Z. Wu, S. Song, K. Mackie, F. Guo, *Lab Chip* **2021**, *21*, 2194.

[50] a) H. M. Poling, D. Wu, N. Brown, M. Baker, T. A. Hausfeld, N. Huynh, S. Chaffron, J. C. Y. Dunn, S. P. Hogan, J. M. Wells, M. A. Helmrath, M. M. Mahe, *Nat. Biomed. Eng.* **2018**, *2*, 429; b) M. Elsaadany, M. Harris, E. Yildirim-Ayan, *Biomed Res. Int.* **2017**, *2017*, 1; c) H. Lv, J. Dong, Y. Qiu, Y. Yang, Y. Zhu, *Lab Chip* **2020**, *20*, 2394.

[51] Y. Li, M. Chen, J. Hu, R. Sheng, Q. Lin, X. He, M. Guo, *Cell Stem Cell* **2020**, *28*, 63.

[52] G. Fang, H. Lu, R. Al-Nakashli, R. Chapman, Y. Zhang, L. A. Ju, G. Lin, M. H. Stenzel, D. Jin, *Biofabrication* **2021**, *14*, 015006.

[53] K. Sakthivel, H. Kumar, M. G. A. Mohamed, B. Talebjedi, J. Shim, H. Najjaran, M. Hoorfar, K. Kim, *Small* **2020**, *16*, e2000941.

[54] A. Desmaison, C. Frongia, K. Grenier, B. Ducommun, V. Lobjois, *PLoS One* **2013**, *8*, e80447.

[55] Yesl Jun, JaeSeo Lee, Seongkyun Choi, Ji Hun Yang, Maike Sander, Seok Chung, S.-H. Lee, *Sci. Adv.* **2019**, *5*, eaax4520.

[56] E. Latorre, S. Kale, L. Casares, M. Gomez-Gonzalez, M. Uroz, L. Valon, R. V. Nair, E. Garreta, N. Montserrat, A. Del Campo, B. Ladoux, M. Arroyo, X. Trepat, *Nature* **2018**, *563*, 203.

[57] K. Alessandri, B. R. Sarangi, V. V. Gurchenkov, B. Sinha, T. R. Kiessling, L. Fetler, F. Rico, S. Scheuring, C. Lamaze, A. Simon, S. Geraldo, D. Vignjevic, H. Domejean, L. Rolland, A. Funfak, J. Bibette, N. Bremond, P. Nassoy, *Proc Natl Acad Sci U S A* **2013**, *110*, 14843.

[58] M. H. Panhwar, F. Czerwinski, V. A. S. Dabbiru, Y. Komaragiri, B. Fregin, D. Biedenweg, P. Nestler, R. H. Pires, O. Otto, *Nat. Commun.* **2020**, *11*, 2190.

[59] a) C. J. Chan, T. Hiiragi, *Development* **2020**, *147*, dev190629; b) A. Trushko, I. Di Meglio, A. Merzouki, C. Blanch-Mercader, S. Abuhattum, J. Guck, K. Alessandri, P. Nassoy, K. Kruse, B. Chopard, A. Roux, *Dev. Cell* **2020**, *54*, 655; c) K. Leonavicius, C. Royer, C. Preece, B. Davies, J. S. Biggins, S. Srinivas, *Proc Natl Acad Sci U S A* **2018**, *115*, 10375.

[60] R. K. Jain, J. D. Martin, T. Stylianopoulos, *Annu. Rev. Biomed. Eng.* **2014**, *16*, 321.

[61] a) T. Stylianopoulos, L. L. Munn, R. K. Jain, *Trends Cancer* **2018**, *4*, 292; b) T. Stylianopoulos, *J. Biomech. Eng.* **2017**, *139*.

[62] G. Fang, H. Lu, L. Rodriguez de la Fuente, A. M. K. Law, G. Lin, D. Jin, D. Gallego-Ortega, *Adv. Sci.* **2021**, *8*, 2102418.

[63] a) D. R. Gossett, H. T. Tse, S. A. Lee, Y. Ying, A. G. Lindgren, O. O. Yang, J. Rao, A. T. Clark, D. Di Carlo, *Proc Natl Acad Sci U S A* **2012**, *109*, 7630; b) P. Memmolo, L. Miccio, F. Merola, M. Mugnano, P. Ferraro, *Frontiers in Physics* **2019**, *7*, 111.

[64] M. W. Tibbitt, K. S. Anseth, *Biotechnol. Bioeng.* **2009**, *103*, 655.

[65] Z. Zhao, C. Vizetto-Duarte, Z. K. Moay, M. I. Setyawati, M. Rakshit, M. H. Kathawala, K. W. Ng, *Front Bioeng Biotechnol* **2020**, *8*, 611.

[66] N. Broguiere, L. Isenmann, C. Hirt, T. Ringel, S. Placzek, E. Cavalli, F. Ringnalda, L. Villiger, R. Zullig, R. Lehmann, G. Rogler, M. H. Heim, J. Schuler, M. Zenobi-Wong, G. Schwank, *Adv. Mater.* **2018**, *30*, 1801621.

[67] R. Curvello, G. Garnier, *Biomacromolecules* **2021**, *22*, 701.

[68] N. Gjorevski, N. Sachs, A. Manfrin, S. Giger, M. E. Bragina, P. Ordonez-Moran, H. Clevers, M. P. Lutolf, *Nature* **2016**, *539*, 560.

[69] M. M. Capeling, M. Czerwinski, S. Huang, Y. H. Tsai, A. Wu, M. S. Nagy, B. Juliar, N. Sundaram, Y. Song, W. M. Han, S. Takayama, E. Alsberg, A. J. Garcia, M. Helmrath, A. J. Putnam, J. R. Spence, *Stem Cell Rep.* **2019**, *12*, 381.

[70] a) G. G. Giobbe, C. Crowley, C. Luni, S. Campinoti, M. Khedr, K. Kretzschmar, M. M. De Santis, E. Zambaiti, F. Michielin, L. Meran, Q. Hu, G. van Son, L. Urbani, A. Manfredi, M. Giomo, S. Eaton, D. Cacchiarelli, V. S. W. Li, H. Clevers, P. Bonfanti, N. Elvassore, P. De Coppi, *Nat. Commun.* **2019**, *10*, 5658; b) R. Simsa, T. Rothenbucher, H. Gurbuz, N. Ghosheh, J. Emneus, L. Jenndahl, D. L. Kaplan, N. Bergh, A. M. Serrano, P. Fogelstrand, *PLoS One* **2021**, *16*, e0245685.

[71] X. Tian, M. E. Werner, K. C. Roche, A. D. Hanson, H. P. Foote, S. K. Yu, S. B. Warner, J. A. Copp, H. Lara, E. L. Wauthier, J. M. Caster, L. E. Herring, L. Zhang, J. E. Tepper, D. S. Hsu, T. Zhang, L. M. Reid, A. Z. Wang, *Nat. Biomed. Eng.* **2018**, *2*, 443.

[72] A. N. Cho, Y. Jin, Y. An, J. Kim, Y. S. Choi, J. S. Lee, J. Kim, W. Y. Choi, D. J. Koo, W. Yu, G. E. Chang, D. Y. Kim, S. H. Jo, J. Kim, S. Y. Kim, Y. G. Kim, J. Y. Kim, N. Choi, E. Cheong, Y. J. Kim, H. S. Je, H. C. Kang, S. W. Cho, *Nat. Commun.* **2021**, *12*, 4730.

[73] Y. Hong, I. Koh, K. Park, P. Kim, *ACS Biomater. Sci. Eng.* **2017**, *3*, 3546.

[74] D. Kim, K. Kim, J. Y. Park, *Lab Chip* **2021**, *21*, 1974.

[75] a) B. R. Lee, J. W. Hwang, Y. Y. Choi, S. F. Wong, Y. H. Hwang, D. Y. Lee, S. H. Lee, *Biomaterials* **2012**, *33*, 837; b) B. Patra, C. C. Peng, W. H. Liao, C. H. Lee, Y. C. Tung, *Sci. Rep.* **2016**, *6*,

21061; c) S. W. Lee, S. Hong, B. Jung, S. Y. Jeong, J. H. Byeon, G. S. Jeong, J. Choi, C. Hwang, *Biotechnol. Bioeng.* **2019**, *116*, 3041.

[76] D. J. Jung, T. H. Shin, M. Kim, C. O. Sung, S. J. Jang, G. S. Jeong, *Lab Chip* **2019**, *19*, 2854.

[77] N. Brandenberg, S. Hoehnel, F. Kuttler, K. Homicsko, C. Ceroni, T. Ringel, N. Gjorevski, G. Schwank, G. Coukos, G. Turcatti, M. P. Lutolf, *Nat. Biomed. Eng.* **2020**, *4*, 863.

[78] T. Tao, Y. Wang, W. Chen, Z. Li, W. Su, Y. Guo, P. Deng, J. Qin, *Lab Chip* **2019**, *19*, 948.

[79] C. X. Zhao, D. Chen, Y. Hui, D. A. Weitz, A. P. J. Middelberg, *ChemPhysChem* **2017**, *18*, 1393.

[80] a) S. Sart, R. F. Tomasi, G. Amselem, C. N. Baroud, *Nat. Commun.* **2017**, *8*, 469; b) H. T. Liu, H. Wang, W. B. Wei, H. Liu, L. Jiang, J. H. Qin, *Small* **2018**, *14*, 1801095.

[81] a) C. Kim, J. Park, J. Y. Kang, *Biomicrofluidics* **2014**, *8*, 066504; b) A. G. Hati, D. C. Bassett, J. M. Ribe, P. Sikorski, D. A. Weitz, B. T. Stokke, *Lab Chip* **2016**, *16*, 3718; c) S. Utech, R. Prodanovic, A. S. Mao, R. Ostafe, D. J. Mooney, D. A. Weitz, *Adv. Healthcare Mater.* **2015**, *4*, 1628.

[82] a) B. Kwak, Y. Lee, J. Lee, S. Lee, J. Lim, *J Control Release* **2018**, *275*, 201; b) H. F. Chan, Y. Zhang, K. W. Leong, *Small* **2016**, *12*, 2720.

[83] a) P. Agarwal, S. Zhao, P. Bielecki, W. Rao, J. K. Choi, Y. Zhao, J. Yu, W. Zhang, X. He, *Lab Chip* **2013**, *13*, 4525; b) Y. C. Lu, W. Song, D. An, B. J. Kim, R. Schwartz, M. Wu, M. Ma, *J. Mater. Chem. B* **2015**, *3*, 353.

[84] a) M. E. Dolega, F. Abeille, N. Picollet-D'hahan, X. Gidrol, *Biomaterials* **2015**, *52*, 347; b) B. Laperrousaz, S. Porte, S. Gerbaud, V. Harma, F. Kermarrec, V. Hourtane, F. Bottausci, X. Gidrol, N. Picollet-D'hahan, *Nucleic Acids Res.* **2018**, *46*, e70.

[85] Y. C. Lu, D. J. Fu, D. An, A. Chiu, R. Schwartz, A. Y. Nikitin, M. Ma, *Adv. Biosyst.* **2017**, *1*, 1700165.

[86] H. Liu, Y. Wang, H. Wang, M. Zhao, T. Tao, X. Zhang, J. Qin, *Adv. Sci. (Weinh)* **2020**, *7*, 1903739.

[87] a) C. Rinoldi, M. Costantini, E. Kijenska-Gawronska, S. Testa, E. Fornetti, M. Heljak, M. Cwiklinska, R. Buda, J. Baldi, S. Cannata, J. Guzowski, C. Gargioli, A. Khademhosseini, W. Swieszkowski, *Adv. Healthcare Mater.* **2019**, *8*, 1801218; b) K. Iijima, S. Ichikawa, S. Ishikawa, D. Matsukuma, Y. Yataka, H. Otsuka, M. Hashizume, *ACS Biomater. Sci. Eng.* **2019**, *5*, 5688; c) M. F. Leong, H. F. Lu, T. C. Lim, K. Narayanan, S. Gao, L. Y. Wang, R. P. Toh, H. Funke, M. H. Abdul Samad, A. C. Wan, J. Y. Ying, *Tissue Eng Part C Methods* **2016**, *22*, 884; d) A. Y. Hsiao, T. Okitsu, H. Onoe, M. Kiyosawa, H. Teramae, S. Iwanaga, T. Kazama, T. Matsumoto, S. Takeuchi, *PLoS One* **2015**, *10*, e0119010.

[88] S. J. Kim, J. Park, H. Byun, Y. W. Park, L. G. Major, D. Y. Lee, Y. S. Choi, H. Shin, *Biomaterials* **2019**, *188*, 198.

[89] Y. Wang, H. Wang, P. Deng, W. Chen, Y. Guo, T. Tao, J. Qin, *Lab Chip* **2018**, *18*, 3606.

[90] Riya Muckom, Xiaoping Bao, Eric Tran, Evelyn Chen, Abirami Murugappan, Jonathan S. Dordick, Douglas S. Clark, D. V. Schaffer, *Sci. Adv.* **2020**, *5*, eaaz1457.

[91] B. J. Jin, S. Battula, N. Zachos, O. Kovbasnjuk, J. Fawlke-Abel, J. In, M. Donowitz, A. S. Verkman, *Biomicrofluidics* **2014**, *8*, 024106.

[92] a) R. Weser, A. Winkler, M. Weihnacht, S. Menzel, H. Schmidt, *Ultrasonics* **2020**, *106*, 106160; b) C. Richard, A. Fakhfouri, M. Colditz, F. Striggow, R. Kronstein-Wiedemann, T. Tonn, M. Medina-Sanchez, O. G. Schmidt, T. Gemming, A. Winkler, *Lab Chip* **2019**, *19*, 4043; c) S. Jin, X. Wei, J. Ren, Z. Jiang, C. Abell, Z. Yu, *Lab Chip* **2020**, *20*, 3104; d) T. Inui, J. Mei, C. Imashiro, Y. Kurashina, J. Friend, K. Takemura, *Lab Chip* **2021**, *21*, 1299.

[93] a) K. Chen, M. Wu, F. Guo, P. Li, C. Y. Chan, Z. Mao, S. Li, L. Ren, R. Zhang, T. J. Huang, *Lab Chip* **2016**, *16*, 2636; b) B. Chen, Y. Wu, Z. Ao, H. Cai, A. Nunez, Y. Liu, J. Foley, K. Nephew, X. Lu, F. Guo, *Lab Chip* **2019**, *19*, 1755.

[94] Z. Ao, H. Cai, Z. Wu, J. Ott, H. Wang, K. Mackie, F. Guo, *Lab Chip* **2021**, *21*, 688.

[95] T. Takebe, B. Zhang, M. Radisic, *Cell Stem Cell* **2017**, *21*, 297.

[96] a) S. Grebenyuk, A. Ranga, *Front Bioeng Biotechnol* **2019**, *7*, 39; b) S. Zhang, Z. Wan, R. D. Kamm, *Lab Chip* **2021**, *21*, 473.

[97] a) J. S. Miller, K. R. Stevens, M. T. Yang, B. M. Baker, D. H. Nguyen, D. M. Cohen, E. Toro, A. A. Chen, P. A. Galie, X. Yu, R. Chaturvedi, S. N. Bhatia, C. S. Chen, *Nat. Mater.* **2012**, *11*, 768; b) D. F. Duarte Campos, C. D. Lindsay, J. G. Roth, B. L. LeSavage, A. J. Seymour, B. A. Krajina, R. Ribeiro, P. F. Costa, A. Blaeser, S. C. Heilshorn, *Front Bioeng Biotechnol* **2020**, *8*, 374; c) B. F. L. Lai, R. X. Z. Lu, L. Davenport Huyer, S. Kakinoki, J. Yazbeck, E. Y. Wang, Q. Wu, B. Zhang, M. Radisic, *Nat. Protoc.* **2021**, *16*, 2158.

[98] a) S. Kim, H. Lee, M. Chung, N. L. Jeon, *Lab Chip* **2013**, *13*, 1489; b) S. Kim, M. Chung, J. Ahn, S. Lee, N. L. Jeon, *Lab Chip* **2016**, *16*, 4189.

[99] a) Y. Nashimoto, R. Okada, S. Hanada, Y. Arima, K. Nishiyama, T. Miura, R. Yokokawa, *Biomaterials* **2020**, *229*, 119547; b) K. Haase, G. S. Offeddu, M. R. Gillrie, R. D. Kamm, *Adv. Funct. Mater.* **2020**, *30*, 2002444; c) S. Oh, H. Ryu, D. Tahk, J. Ko, Y. Chung, H. K. Lee, T. R. Lee, N. L. Jeon, *Lab Chip* **2017**, *17*, 3405; d) J. Ko, J. Ahn, S. Kim, Y. Lee, J. Lee, D. Park, N. L. Jeon, *Lab Chip* **2019**, *19*, 2822; e) I. Salmon, S. Grebenyuk, A. R. Abdel Fattah, G. Rustandi, T. Pilkington, C. Verfaillie, A. Ranga, *Lab Chip* **2022**, *22*, 1615.

[100] a) Y. Jin, J. Kim, J. S. Lee, S. Min, S. Kim, D.-H. Ahn, Y.-G. Kim, S.-W. Cho, *Adv. Funct. Mater.* **2018**, *28*, 1801954; b) T. Takebe, K. Sekine, M. Enomura, H. Koike, M. Kimura, T. Ogaeri, R. R. Zhang, Y. Ueno, Y. W. Zheng, N. Koike, S. Aoyama, Y. Adachi, H. Taniguchi, *Nature* **2013**, *499*, 481.

[101] a) R. A. Wimmer, A. Leopoldi, M. Aichinger, N. Wick, B. Hantusch, M. Novatchkova, J. Taubenschmid, M. Hammerle, C. Esk, J. A. Bagley, D. Lindenhofer, G. Chen, M. Boehm, C. A. Agu, F. Yang, B. Fu, J. Zuber, J. A. Knoblich, D. Kerjaschki, J. M. Penninger, *Nature* **2019**, *565*, 505; b) F. Wu, D. Wu, Y. Ren, Y. Huang, B. Feng, N. Zhao, T. Zhang, X. Chen, S. Chen, A. Xu, *J. Hepatol.* **2019**, *70*, 1145.

[102] S. Rajasekar, D. S. Y. Lin, L. Abdul, A. Liu, A. Sotra, F. Zhang, B. Zhang, *Adv. Mater.* **2020**, *32*, 2002974.

[103] a) A. A. Mansour, J. T. Goncalves, C. W. Bloyd, H. Li, S. Fernandes, D. Quang, S. Johnston, S. L. Parylak, X. Jin, F. H. Gage, *Nat. Biotechnol.* **2018**, *36*, 432; b) M. A. Lancaster, *Nat. Biotechnol.* **2018**, *36*, 407.

[104] a) B. F. L. Lai, R. X. Z. Lu, Y. Hu, L. Davenport Huyer, W. Dou, E. Y. Wang, N. Radulovich, M. S. Tsao, Y. Sun, M. Radisic, *Adv. Funct. Mater.* **2020**, *30*, 2000545; b) C. Kim, J. Kasuya, J. Jeon, S. Chung, R. D. Kamm, *Lab Chip* **2015**, *15*, 301.

[105] a) K. Yuki, N. Cheng, M. Nakano, C. J. Kuo, *Trends Immunol.* **2020**, *41*, 652; b) C. P. Miller, W. Shin, E. H. Ahn, H. J. Kim, D. H. Kim, *Trends Biotechnol.* **2020**, *38*, 857.

[106] a) R. W. Jenkins, A. R. Aref, P. H. Lizotte, E. Ivanova, S. Stinson, C. W. Zhou, M. Bowden, J. Deng, H. Liu, D. Miao, M. X. He, W. Walker, G. Zhang, T. Tian, C. Cheng, Z. Wei, S. Palakurthi, M. Bittinger, H. Vitzthum, J. W. Kim, A. Merlino, M. Quinn, C. Venkataramani, J. A. Kaplan, A. Portell, P. C. Gokhale, B. Phillips, A. Smart, A. Rotem, R. E. Jones, et al., *Cancer Discov* **2018**, *8*, 196; b) A. R. Aref, M. Campisi, E. Ivanova, A. Portell, D. Larios, B. P. Piel, N. Mathur, C. Zhou, R. V. Coakley, A. Bartels, M. Bowden, Z. Herbert, S. Hill, S. Gilhooley, J. Carter, I. Canadas, T. C. Thai, S. Kitajima, V. Chiono, C. P. Paweletz, D. A. Barbie, R. D. Kamm, R. W. Jenkins, *Lab Chip* **2018**, *18*, 3129.

[107] S. W. L. Lee, G. Adriani, E. Ceccarello, A. Pavesi, A. T. Tan, A. Bertoletti, R. D. Kamm, S. C. Wong, *Front Immunol* **2018**, *9*, 416.

[108] J. M. Ayuso, R. Truttschel, M. M. Gong, M. Humayun, M. Virumbrales-Munoz, R. Vitek, M. Felder, S. D. Gillies, P. Sondel,

K. B. Wisinski, M. Patankar, D. J. Beebe, M. C. Skala, *Oncoimmunology* **2019**, *8*, 1553477.

[109] R. F. Tomasi, S. Sart, T. Champetier, C. N. Baroud, *Cell Rep.* **2020**, *31*, 107670.

[110] X. Yue, T. D. Nguyen, V. Zellmer, S. Zhang, P. Zorlutuna, *Biomaterials* **2018**, *170*, 37.

[111] a) D. D. Truong, A. Kratz, J. G. Park, E. S. Barrientos, H. Saini, T. Nguyen, B. Pockaj, G. Mouneimne, J. LaBaer, M. Nikkhah, *Cancer Res.* **2019**, *79*, 3139; b) D. Ohlund, A. Handly-Santana, G. Biffi, E. Elyada, A. S. Almeida, M. Ponz-Sarvise, V. Corbo, T. E. Oni, S. A. Hearn, E. J. Lee, I. I. Chio, C. I. Hwang, H. Tiriac, L. A. Baker, D. D. Engle, C. Feig, A. Kultti, M. Egeblad, D. T. Fearon, J. M. Crawford, H. Clevers, Y. Park, D. A. Tuveson, *J. Exp. Med.* **2017**, *214*, 579; c) M. F. Estrada, S. P. Rebelo, E. J. Davies, M. T. Pinto, H. Pereira, V. E. Santo, M. J. Smalley, S. T. Barry, E. J. Gualda, P. M. Alves, E. Anderson, C. Brito, *Biomaterials* **2016**, *78*, 50; d) Q. Sun, S. H. Tan, Q. Chen, R. Ran, Y. Hui, D. Chen, C.-X. Zhao, *ACS Biomater. Sci. Eng.* **2018**, *4*, 4425; e) L. Zhang, K. Chen, H. Zhang, B. Pang, C. H. Choi, A. S. Mao, H. Liao, S. Utech, D. J. Mooney, H. Wang, D. A. Weitz, *Small* **2018**, *14*, 1702955; f) K. Shik Mun, K. Arora, Y. Huang, F. Yang, S. Yarlagadda, Y. Ramananda, M. Abu-El-Haija, J. J. Palermo, B. N. Appakalai, J. D. Nathan, A. P. Naren, *Nat. Commun.* **2019**, *10*, 3124; g) S. Chen, A. Giannakou, S. Wyman, J. Gruzas, J. Golas, W. Zhong, C. Loreth, L. Sridharan, T.-T. Yamin, M. Damelin, K. G. Geles, *Proc. Natl. Acad. Sci. USA* **2018**, *115*, E11671.

[112] M. Verhulsel, A. Simon, M. Bernheim-Dennery, V. R. Gannavarapu, L. Geremie, D. Ferraro, D. Krndija, L. Talini, J. L. Viovy, D. M. Vignjevic, S. Descroix, *Lab Chip* **2021**, *21*, 365.

[113] a) M. T. Ghoneim, A. Nguyen, N. Dereje, J. Huang, G. C. Moore, P. J. Murzynowski, C. Dagdeviren, *Chem. Rev.* **2019**, *119*, 5248; b) L. Manjakkal, S. Dervin, R. Dahiya, *RSC Adv.* **2020**, *10*, 8594; c) L. Manjakkal, D. Szwagierczak, R. Dahiya, *Prog. Mater. Sci.* **2020**, *109*.

[114] a) M. E. Gray, J. R. K. Marland, C. Dunare, E. O. Blair, J. Meehan, A. Tsiamis, I. H. Kunkler, A. F. Murray, D. Argyle, A. Dyson, M. Singer, M. A. Potter, *Am J Physiol Gastrointest Liver Physiol* **2019**, *317*, G242; b) L. Rivas, S. Dulay, S. Miserere, L. Pla, S. B. Marin, J. Parra, E. Eixarch, E. Gratacos, M. Illa, M. Mir, J. Samitier, *Biosens. Bioelectron.* **2020**, *153*, 112028; c) A. Moya, M. Ortega-Ribera, X. Guimera, E. Sowade, M. Zea, X. Illa, E. Ramon, R. Villa, J. Gracia-Sancho, G. Gabriel, *Lab Chip* **2018**, *18*, 2023.

[115] a) L. Wang, M. Xu, Y. Xie, C. Qian, W. Ma, L. Wang, Y. Song, *Sens. Actuators, B* **2019**, *285*, 264; b) M. H. Asif, A. Razaq, N. Akbar, B. Danielsson, I. Sultana, *Mater. Res. Express* **2019**, *6*; c) W. Lipińska, K. Siuzdak, J. Karczewski, A. Dołęga, K. Grochowska, *Sens. Actuators, B* **2020**, *330*, 129409.

[116] P. M. Misun, J. Rothe, Y. R. F. Schmid, A. Hierlemann, O. Frey, *Microsyst. Nanoeng.* **2016**, *2*, 16022.

[117] a) G. Cappi, F. M. Spiga, Y. Moncada, A. Ferretti, M. Beyeler, M. Bianchessi, L. Decosterd, T. Buclin, C. Guiducci, *Anal. Chem.* **2015**, *87*, 5278; b) F. Real-Fernandez, G. Rossi, F. Lolli, A. M. Papini, P. Rovero, *MethodsX* **2015**, *2*, 141.

[118] S. R. Shin, Y. S. Zhang, D. J. Kim, A. Manbohi, H. Avci, A. Silvestri, J. Aleman, N. Hu, T. Kilic, W. Keung, M. Righi, P. Assawes, H. A. Alhadrami, R. A. Li, M. R. Dokmeci, A. Khademhosseini, *Anal. Chem.* **2016**, *88*, 10019.

[119] R. K. Jayne, M. C. Karakan, K. Zhang, N. Pierce, C. Michas, D. J. Bishop, C. S. Chen, K. L. Ekinci, A. E. White, *Lab Chip* **2021**, *21*, 1724.

[120] D. S. Kim, Y. W. Choi, A. Shanmugasundaram, Y. J. Jeong, J. Park, N. E. Oyunbaatar, E. S. Kim, M. Choi, D. W. Lee, *Nat. Commun.* **2020**, *11*, 535.

[121] Q. Li, K. Nan, P. Le Floch, Z. Lin, H. Sheng, T. S. Blum, J. Liu, *Nano Lett.* **2019**, *19*, 5781.

[122] H. Liu, O. A. Bolonduro, N. Hu, J. Ju, A. A. Rao, B. M. Duffy, Z. Huang, L. D. Black, B. P. Timko, *Nano Lett.* **2020**, *20*, 2585.

[123] Anna Kalmykov, Changjin Huang, Jacqueline Bliley, Daniel Shiwarski, Joshua Tashman, Arif Abdullah, Sahil K. Rastogi, Shivani Shukla, Elnatan Mataev, Adam W. Feinberg, K. Jimmy Hsia, T. Cohen-Karni, *Sci. Adv.* **2019**, *5*.

[124] K. F. Lei, W. W. Ji, A. Goh, C. H. Huang, M. Y. Lee, *Biomed. Microdevices* **2019**, *21*, 94.

[125] Z. Ao, H. Cai, Z. Wu, J. Krzesniak, C. Tian, Y. Y. Lai, K. Mackie, F. Guo, *Anal. Chem.* **2022**, *94*, 1365.

[126] Y. Y. Chen, P. N. Silva, A. M. Syed, S. Sindhwani, J. V. Rocheleau, W. C. W. Chana, *Proc. Natl. Acad. Sci.* **2017**, *114*, E1036.

[127] a) M. Roy, D. Seo, S. Oh, J. W. Yang, S. Seo, *Biosens. Bioelectron.* **2017**, *88*, 130; b) A. Greenbaum, A. Feizi, N. Akbari, A. Ozcan, *Opt. Express* **2013**, *21*, 12469; c) Y. Zhang, Y. Shin, K. Sung, S. Yang, H. Chen, H. Wang, D. Teng, Y. Rivenson, R. P. Kulkarni, A. Ozcan, *Sci. Adv.* **2017**, *3*; d) S. Jiang, M. Guan, J. Wu, G. Fang, X. Xu, D. Jin, Z. Liu, K. Shi, F. Bai, S. Wang, P. Xi, *Advanced Photonics* **2020**, *2*.

[128] V. Bianco, B. Mandracchia, V. Marchesano, V. Pagliarulo, F. Olivieri, S. Coppola, M. Paturzo, P. Ferraro, *Light Sci Appl* **2017**, *6*, e17055.

[129] Z. Luo, A. Yurt, R. Stahl, M. S. Carlon, A. S. Ramalho, F. Vermeulen, A. Lambrechts, D. Braeken, L. Lagae, *Opt. Express* **2020**, *28*, 26935.

[130] Ø. I. Helle, F. T. Dullo, M. Lahrberg, J.-C. Tinguely, O. G. Hellesø, B. S. Ahluwalia, *Nat. Photonics* **2020**, *14*, 431.

[131] R. Diekmann, Ø. I. Helle, C. I. Øie, P. McCourt, T. R. Huser, M. Schüttpelz, B. S. Ahluwalia, *Nat. Photonics* **2017**, *11*, 322.

[132] a) Y. J. Fan, H. Y. Hsieh, S. F. Tsai, C. H. Wu, C. M. Lee, Y. T. Liu, C. H. Lu, S. W. Chang, B. C. Chen, *Lab Chip* **2021**, *21*, 344; b) A. Beghin, G. Grenci, G. Sahni, S. Guo, H. Rajendiran, T. Delaire, S. B. Mohamad Raffi, D. Blanc, R. de Mets, H. T. Ong, X. Galindo, A. Monet, V. Acharya, V. Racine, F. Levet, R. Galland, J.-B. Sibarita, V. Viasnoff, *Nat. Methods* **2022**, *18*, 881.

[133] a) P. Bon, J. Linares-Loyez, M. Feyeux, K. Alessandri, B. Lounis, P. Nassoy, L. Cognet, *Nat. Methods* **2018**, *15*, 449; b) Y. Liu, F. Wang, H. Lu, G. Fang, S. Wen, C. Chen, X. Shan, X. Xu, L. Zhang, M. Stenzel, D. Jin, *Small* **2020**, *16*, e1905572; c) C. Chen, F. Wang, S. Wen, Q. P. Su, M. C. L. Wu, Y. Liu, B. Wang, D. Li, X. Shan, M. Kianinia, I. Aharonovich, M. Toth, S. P. Jackson, P. Xi, D. Jin, *Nat. Commun.* **2018**, *9*, 3290; d) Y. Liu, F. Wang, H. Lu, S. Wen, C. Chen, X. Shan, G. Fang, D. Jin, *Enhanced Spectroscopies and Nanoimaging* **2020**, *11468*, 11468G.

[134] a) S. Min, S. Kim, S. W. Cho, *Exp. Mol. Med.* **2020**, *52*, 227; b) Y. S. Son, S. J. Ki, R. Thanavel, J. J. Kim, M. O. Lee, J. Kim, C. R. Jung, T. S. Han, H. S. Cho, C. M. Ryu, S. H. Kim, D. S. Park, M. Y. Son, *FASEB J.* **2020**, *34*, 9899; c) A. M. K. Law, L. Rodriguez de la Fuente, T. J. Grundy, G. Fang, F. Valdes-Mora, D. Gallego-Ortega, *Front Oncol* **2021**, *11*, 782766.

[135] a) C. Gong, F. Sun, G. Yang, C. Wang, C. Huang, Y. C. Chen, *Laser Photonics Rev.* **2022**, *16*; b) H. Kavand, R. Nasiri, A. Herland, *Adv. Mater.* **2022**, *34*, 2107876.

[136] A. Herland, B. M. Maoz, D. Das, M. R. Somayaji, R. Prantil-Baun, R. Novak, M. Cronce, T. Huffstater, S. S. F. Jeanty, M. Ingram, A. Chalkiadaki, D. Benson Chou, S. Marquez, A. Delahanty, S. Jalili-Firoozinezhad, Y. Milton, A. Sontheimer-Phelps, B. Swenor, O. Levy, K. K. Parker, A. Przekwas, D. E. Ingber, *Nat. Biomed. Eng.* **2020**, *4*, 421.

[137] a) D. Bovard, A. Sandoz, K. Luettich, S. Frentzel, A. Iskandar, D. Marescotti, K. Trivedi, E. Guedj, Q. Dutertre, M. C. Peitsch, J. Hoeng, *Lab Chip* **2018**, *18*, 3814; b) E. Ferrari, M. Rasponi, *APL Bioeng.* **2021**, *5*, 031505; c) J. Theobald, A. Ghanem, P. Wallisch, A. A. Banaeiyan, M. A. Andrade-Navarro, K. Taskova, M. Haltmeier,

Yu-Cheng Chen received his Ph.D. degree from the University of Michigan, Ann Arbor and joined Nanyang Technological University Singapore as a principal investigator in 2018. His research focuses on the development of novel functional bio-lasers, from molecular to multicellular models, thriving hard to advance this new technology to the clinical field. His work on optofluidics and biological lasers has been highly recognized by MIT Under 35 Innovators (Asia-Pacific).

Hongxu Lu obtained his Ph.D. from the University of Tsukuba in 2009. Then, he received postdoctoral training at the National Institute for Materials Science of Japan and the University of New South Wales (UNSW). Since 2015, he has worked as a research fellow at UNSW the University of Technology Sydney, and the University of Sydney. He joined the Shanghai Institute of Ceramics Chinese Academy of Science as a principal investigator in 2022. His current research focuses on developing organoid and organ-on-chips models combining bioactive materials, stem cells, 3D in vitro culture, and microfluidic technology.

Dayong Jin received his Ph.D. from Macquarie University in 2007. At Macquarie, he was promoted to Lecturer in 2010, Associate Professor in 2014 and Professorial Fellow in 2015. He joined the University of Technology Sydney in 2015, as a Chair Professor, to lead its research in Materials and Technology and to establish the Institute for Biomedical Materials and Devices (IBMD), of which he is the director. His current research focuses on biomedical engineering, biophotonics, analytical chemistry, and instrumental physics.

2215043 (19 of 19)